D3.1 BURNT AREA AND HIGH FIRE RISK MAPS. MAPS OF BURNT AREA AND HIGH FIRE RISK ZONES AT EACH REPLICATED LANDSCAPE

Planned delivery date (as in DoA): M16

Due date of deliverable: January 2025

Delivered: June 2025

Work Package: WP3

Deliverable leader: UNITO

CUP number: 2022R7F259

REWILDFIRE — PIANO NAZIONALE DI RIPRESA E RESILIENZA (PNRR)

Missione 4 “Istruzione e Ricerca” - Componente C2

Investimento 1.1, “Fondo per il Programma Nazionale di Ricerca e Progetti di Rilevante Interesse Nazionale (PRIN)”

Project Acronym: REWILDFIRE

Rewilding policies for carbon sequestration under increasing fire risk

Duration of the project: September 28, 2023 – February 28, 2025

CITATION:

Spadoni G.L., Rainsford F., Passamani C., Djacenko S., Oggioni S., Vacchiano G., Ascoli D. (2026). D3.1 Fire and carbon dynamics simulation. Missione 4 “Istruzione e Ricerca” - Componente C2 Investimento 1.1, “Fondo per il Programma Nazionale di Ricerca e Progetti di Rilevante Interesse Nazionale (PRIN)”, Project REWILDFIRE.

ACKNOWLEDGEMENTS

DISCLAIMER

Table of Contents

Executive Summary

Deliverable 3.1 (WP3) outlines the methodology and key findings from wildfire simulations developed within the REWILD-FIRE project. The goal is to assess the potential of rewilding strategies (afforestation and proforestation) in Alpine environments, while considering for trade-offs with increasing wildfire risk. This work adapts and extends the REMAINS landscape model (pixel-based, 30 × 30 m; see Deliverable 1.1), using time since abandonment (TSA) as a proxy for both age and fuel load dynamics.

The study focused on four representative landscapes of Italian Alpine ecoregions (~50 km^2 each), parameterized along gradients of flammability and land-use abandonment. Fire data were derived from a national wildfire perimeter dataset (2007–2024), used to calibrate annual burned area (BA) and fire-size distributions. To incorporate future climate impacts, the deliverable projects expected BA distributions for 2025–2100 by linking observed BA to seasonal Fire Weather Index (FWI; Copernicus/CEMS) metrics through ridge regression, considering landscape effects. The worst-case climatic scenario (i.e., HadGEM RCP8.5) was used to parameterize fire.

The fire module integrates: (i) spatial fire-risk maps (hazard × damage), (ii) semi-stochastic fire spread with rates dependent on slope and susceptibility, (iii) three suppression/prevention mechanisms (fuel suppression, agro-mosaic, and firebreaks (the latter introduced as a novel component), and (iv) post-fire effects including land-cover transitions and forest "rejuvenation" through age-class reduction.

Four policy scenarios were compared: Business as Usual (BAU), Strict Rewilding with enhanced Suppression (StR_S), Fire-Smart Rewilding with Direct Prevention (FSR_DP), and Fire-Smart Rewilding with Direct and Indirect Prevention (FSR_DIP).

BAU generally resulted in the highest total burned area, while FSR_DIP and FSR_DP produced the lowest BA, particularly in the most fire-prone landscape. FSR_DIP also maintained lower forest ages, due to the combined effects of agro-mosaic and prevention, underscoring the "fire-smart" trade-off. This approach reduces wildfire risk but may limit extensive forest ageing and proforestation. Multivariate analyses suggest that recurrent fires can rejuvenate landscapes over time, lowering mean forest age and potentially hindering carbon stock accumulation.

In conclusion, the deliverable suggests that fire-smart strategies — targeting lower-hazard areas for rewilding and integrating firebreaks with agro-mosaic management — are most effective in preserving the climate benefits of rewilding under rising wildfire risk. However, it also acknowledges the model's sensitivity and limitations in the current modified parameterization of the REMAINS model.

Keywords

Fire risk, Rewilding, Modelling, Fire prevention.

Acronyms

BA: Burned Area (or Burnt Area)

BA_TOT: Total Burned Area

BAU: Business as Usual

CDR: Carbon Dioxide Removal

FSR_DP: Fire Smart Rewilding and Direct Prevention

FSR_DIP: Fire Smart Rewilding and Direct and Indirect Prevention

LCC: Land Cover Change

LCT: Land Cover Type

PCA: Principal Component Analysis

SR: Spread Rate (fire spread-rate parameter)

StR_S: Strict Rewilding and Suppression

TSA: Time Since Abandonment

Definitions

- **Fire risk**: the expected impact of a wildfire at cell level, defined as Fire Risk = Fire Hazard × Potential Damage.
- **Fire hazard**: the likelihood and potential intensity of fire spread, computed as the product of ignition probability × a slope-derived topographic multiplier × fire susceptibility.
- **Fire danger**: the likelihood that a fire occurs in a given period as a consequence of predisposing fire weather, i.e. dry and windy conditions.
- **Potential damage**: the expected damage if a fire occurs at cell level (paired with fire hazard in the risk formulation).
- **Fire susceptibility**: the effective flammability after accounting for (i) LCT age effects and (ii) management; in the deliverable it is summarised as:
    - aging LCTs (except broadleaf): flammability × linear multiplier (1.4) per age class
    - broadleaf aging LCTs: flammability × exponential multiplier per age class
    - managed LCTs: flammability − 0.3
- **Wildfire event**: each fire starts from a single ignition cell chosen probabilistically from the fire-risk layer; by definition, ignitions occur only in flammable LCTs and outside firebreaks; spread uses an 8-neighbour (queen's case) rule on the 30×30 m grid.
- **Spread Rate (SR)**: a cell-level parameter expressing the relative potential for propagation from a burning cell to a neighbour; SR is defined as a linear combination of slope effects and fire susceptibility**.**
- **Fire suppression mechanisms**: suppression is modelled with three cell-level mechanisms—Fuel suppression**,** Mosaic suppression**,** Firebreak suppression—and firebreak suppression is explicitly presented as an innovation added for REWILDFIRE.
- **Fuel suppression**: a cell is suppressed when SR < fuel.th; SR below the threshold represents *low-intensity behaviour* that can be controlled by firefighting.
- **Mosaic suppression**: suppression occurs when the fire front encounters sufficient agricultural continuity, expressed as a minimum number of consecutive crop cells (mosaic.th, set to 2 in all scenarios).
- **Firebreak suppression**: cells designated as firebreaks stop spread; it has priority over mosaic and fuel suppression (and mosaic has priority over fuel).
- **Rewilding**: an intentional, i.e., planned, passive management strategy leaving vegetation to two main dynamics: (i) afforestation: the dynamic of transition from crop and pasture to forests; (ii) the stop of forest management activities leading to forest aging (proforestation). In REWILDFIRE, rewilding areas increase in age by one year per simulation year ("unitary aging").
- **No management**: differs from rewilding because it is not intentional, even though it also undergoes unitary aging.
- **Strict rewilding**: rewilding allocation strategy prioritising areas in a sequence of pools (protected/unprotected; unmanaged/managed), with expansion via buffers from protected areas if needed.
- **Fire-smart rewilding**: same as strict rewilding, plus the rule that rewilding established in previously managed areas within Protected Areas ('Rwm') cannot be placed on pixels whose unmanaged flammability exceeds 0.7.

1. Introduction

Work Package 3 (WP3) of the REWILD-FIRE project focuses on simulating fires and carbon dynamics, under different management and climate scenarios, with REMAINS landscape model. Within Task 3.1, the model was parameterized to assess trade-offs between fire risk and rewilding strategies across multiple policy scenarios. Landscape dynamics were simulated over 80 years across 4 representative landscapes, each corresponding to distinct Alpine ecoregions.

1.1 Introduction to REMAINS

Achieving net-zero greenhouse gas emissions requires effective carbon dioxide removal (CDR) strategies. In the Alpine region, rewilding through natural afforestation and proforestation is a promising approach to enhance carbon sinks. However, these strategies might also increase wildfire risks, which could lead to carbon losses. The REWILD-FIRE project developed a modified version of the REMAINS model (Duane et al., 2016; Pais et, al. 2023) to assess the trade-offs between forest growth and wildfire risks under different land-use scenarios driven by integrated policies and climate change. Since REMAINS is a process-based model suited for simulating rewilding and fire management policies, and is implemented in the R programming language, it was selected for use within the REWILD-FIRE project. With the agreement of the original developer, the source code was modified and adapted to meet the specific objectives of the project.

REMAINS is a landscape model which simultaneously simulates land cover changes, fire, and landscape management strategies, including fire management approaches. The model is composed by three modules: fire module, vegetation dynamics module, and land use change module (Figure 1). The model is pixel based (30x30m grid) and each pixel is associated with a land cover type, and a time since change value (or 'age'), where changes are due to simulated land cover changes or fires. Time since change is assumed as a proxy for biomass content and, consequently, for carbon stock. All simulated processes and management affect both land cover type and on the time since change, albeit in different ways.

To implement the REWILD-FIRE hypotheses, experiment design and project goals, several innovations were introduced into the functioning of REMAINS. These modifications enable the simulation of the processes and strategies required to address the research questions of the REWILDFIRE project. The introduced innovations are detailed in the following sections of this report.

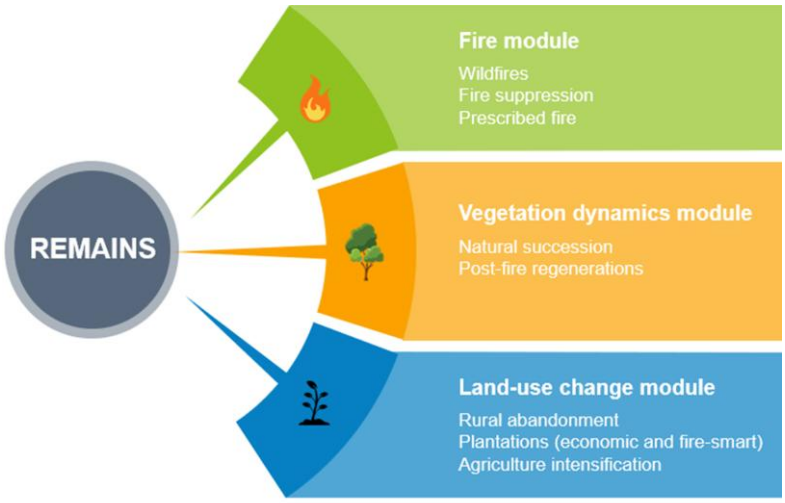

Figure 1. REMAINS model structure.

1.2 Fire process simulation functioning

In the REMAINS modelling framework, wildfire dynamics are simulated within the fire module (Fig. 1), through a spatially explicit, semi-stochastic model operating at annual time steps, as built by Duane et al. (2016). Fire dynamics are simulated in the REMAINS sub-models 'wildfire' and 'fire.risk'. The first sub-model regulates the spread and size of fires, while the second locates fire ignition points. Within the REWILDFIRE project, we modified or expanded these two functions to address specific project's goals, as it will be detailed in the next section. Along with the functions editing, we also did a different data calibration and introduced the simulation of landscape and fire management strategies. These include forest and agropastoral management, rewilding, direct fire prevention through the establishment of firebreaks, and indirect fire prevention through the extension of the agricultural mosaic. The implementation of these innovative strategies within REMAINS will also be described in the following sections. Before introducing the functioning of fire risk and wildfire models, it is worth describing the fire input data needed to run the simulations.

2. Methods

2.1 Study areas

We implemented REMAINS across four different landscapes (Figure 2) covering the Italian alpine region. Each landscape represents a different ecoregion (Figure 2), and so a different social-ecological context. In addition, the landscapes represent gradients of flammability and land use abandonment, increasing from east to west (Table 1), while precipitation and humidity increase in the opposite direction.

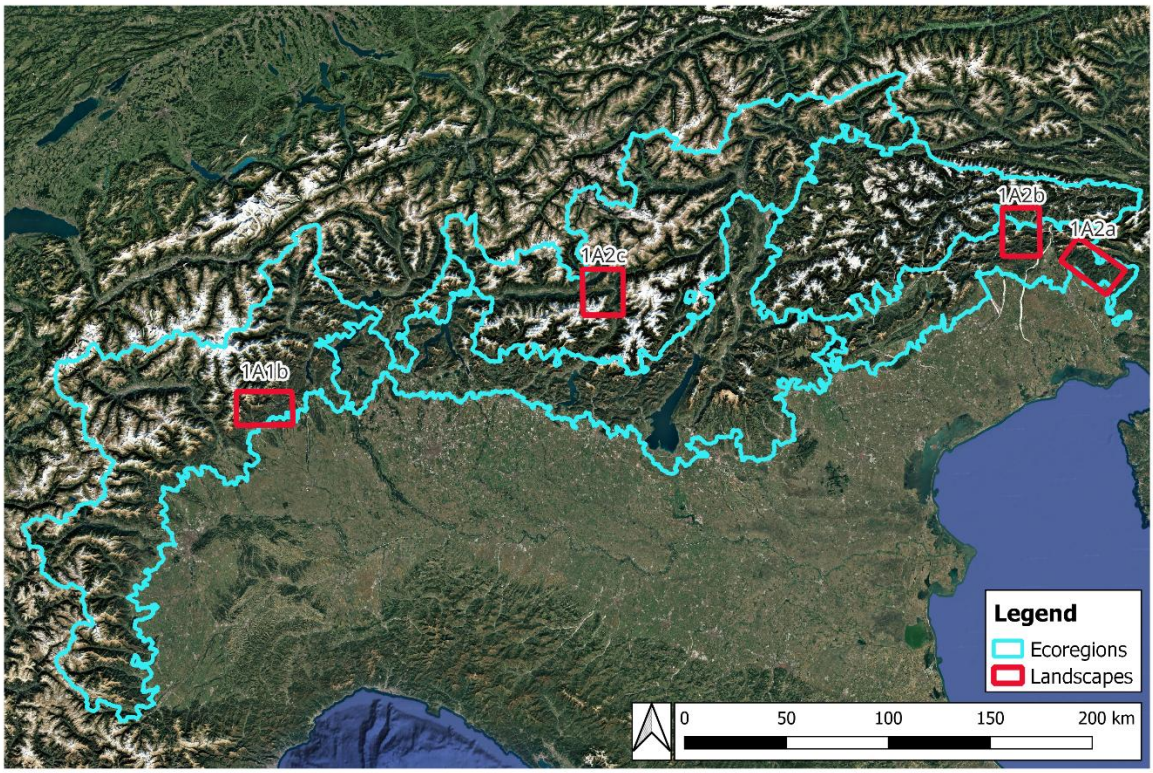

Figure 2. Alpine Ecoregions and Landscapes used for the REWILD-FIRE project.

Table 1. Landscapes features. The meaning of each variable is explained in text.

Variable Type	Variable	Unit	1A1b	1A2a	1A2b	1A2c
Total land	Landscape surface	ha	45144	41855	43418	44642
Land cover type	barren	ha	160.92	111.15	664.11	133.02
	broadleaf	ha	29348.55	34036.74	30060.18	15737.04
	conifer	ha	3958.02	836.1	6284.97	15946.74
	crop	ha	386.46	1502.28	321.21	859.68
	pasture	ha	3905.82	2338.65	3003.39	3771.72
	shrub	ha	3346.92	1261.8	1351.35	3624.12
	sparse	ha	134.28	7.11	398.79	2587.95
	urban	ha	3707.82	1645.02	1160.19	1258.74
	water	ha	195.12	116.55	174.06	722.52
Land cover type	barren	%	0.36	0.27	1.53	0.30
	broadleaf	%	65.01	81.32	69.23	35.25
	conifer	%	8.77	2.00	14.48	35.72
	crop	%	0.86	3.59	0.74	1.93
	pasture	%	8.65	5.59	6.92	8.45
	shrub	%	7.41	3.01	3.11	8.12
	sparse	%	0.30	0.02	0.92	5.80
	urban	%	8.21	3.93	2.67	2.82
	water	%	0.43	0.28	0.40	1.62
Burnable land		ha	40945.77	39975.57	41021.1	39939.3
		%	90.70	95.51	94.48	89.47
Firebreaks		ha	819	800	820	799
Protected area		ha	9189.81	4532.49	4302.18	8485.56
		%	20.36	10.83	9.91	19.01
Initial management	forest_30%	ha	9991.89	10461.78	10903.5	9505.08
	forest_40%	ha	13322.61	13949.1	14538.06	12673.44
	pasture_20%	ha	781.11	467.73	600.66	754.29
	crop_100%	ha	386.46	1502.28	321.21	859.68
Initial management in protected areas	forest_30%	ha	837	763.2	1187.82	898.92
	forest_40%	ha	1100.61	976.95	1594.08	1226.7
	pasture_20%	ha	298.8	42.84	103.5	119.07
	crop_100%	ha	28.08	17.19	4.5	36.36
Rewilding	rw	ha	4069.35	3393.9	2526.48	4166.73
	rwm	ha	0	454.14	1583.37	0
	rwu	ha	0	0	0	0
Rewilding fire smart	fs_rw	ha	4069.35	3393.9	2526.48	4166.73
	fs_rwm	ha	0	454.14	1450.98	0
	fs_rwu	ha	0	0	132.39	0

2.2 Fire Input Data

Fire input data were derived from an Italian national dataset containing all wildfire perimeters recorded by local authorities between 2007 and 2024 (Moris et al., 2024). The landscapes were chosen to represent a gradient of fire activity (Figure 3; Figure 4; Table 2).

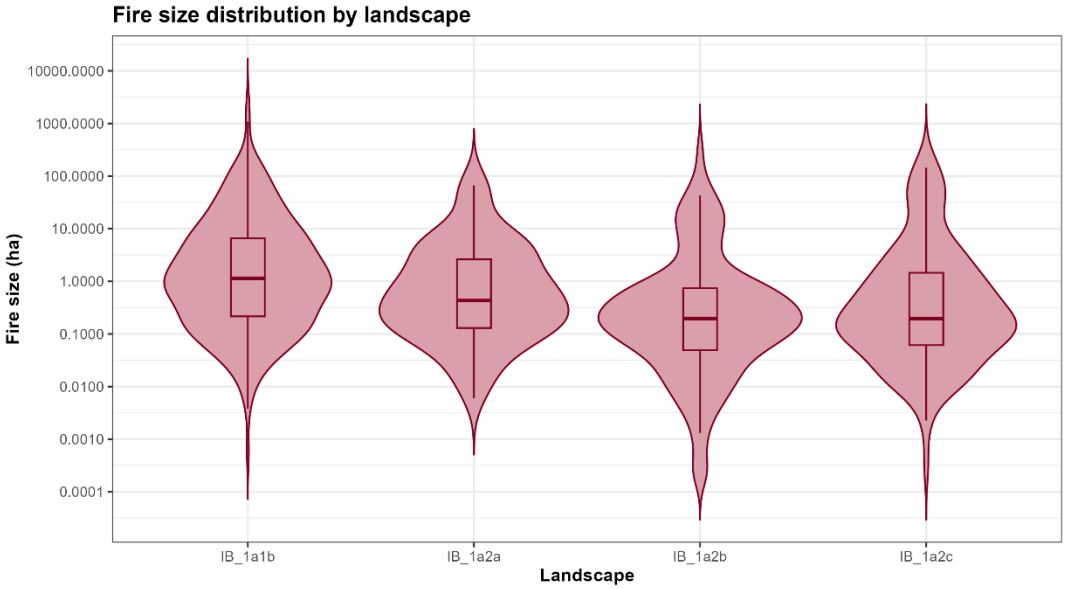

Figure 3. Fire size distribution (in hectares, log scale) derived from the Italian national dataset (2007-2024), considering fires occurring within each landscape or within a 5 km buffer around it.

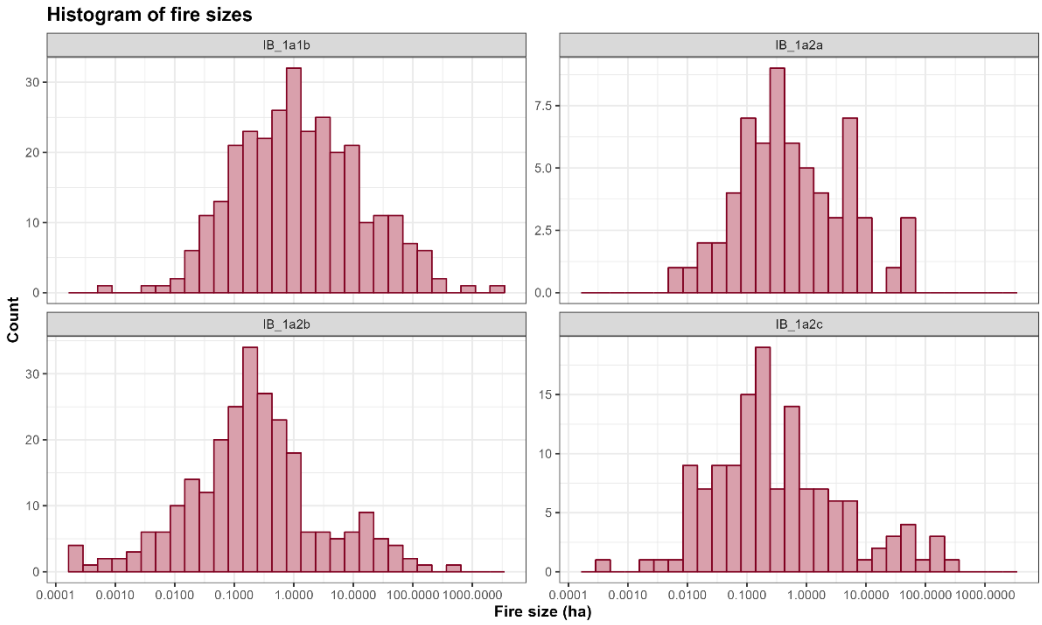

Figure 4. Number of fire events per size class (log scale).

Table 2. Fire characteristics of the landscapes during 2007–2024.

Landscape	n_fires	min_ha	median_ha	mean_ha	max_ha	sd_ha
1a1b	297	5.7E-04	1.14	22.66	2181.22	143.91
1a2a	64	6.0E-03	0.43	4.71	66.47	13.14
1a2b	252	1.8E-04	0.20	5.67	376.68	28.99
1a2c	134	3.2E-04	0.20	8.40	211.18	28.86

2.1.1. Burnt area and Fire size distributions.

Burnt area distribution quantifies the frequency of occurrence of a given total yearly burned area across the calibration period (2007-2024) for each landscape. The frequency interval of the yearly burnt area was set as 100 ha year^{-1}. Fire size distribution, on the other hand, represents the frequency of individual fire events, with a frequency interval of 10 ha year^{-1}. Following the approach of Duane et al. (2016), burnt area distribution was calibrated at the landscape (study area) level, while fire size distribution was calibrated at the ecoregion level to better capture the characteristics of the fire regime. Since the fire size distribution also included the largest fires within each ecoregion, we intentionally selected landscapes located in the most fire-prone areas of each ecoregion, based on the historical fire locations documented in the national dataset 2007-2024. Further enhancement of burnt area distribution was achieved by incorporating the potential impacts from climate change (see chapter 2.1.2.).

2.1.2. Generated future burned area distributions for REMAINS landscapes

Fire Weather Index (FWI) is a widely used indicator of meteorological fire danger (Shmuel et al. 2025). A key practical question is whether changes in FWI translate into comparable changes in burned area (BA) at regional scale (for example, Di Nunno and Granata, 2025). Such question should be addressed by keeping in mind that climate change can alter not only average conditions, but also the frequency and intensity of extreme fire weather (Seneviratne et al. 2021), which are often the major responsible for yearly burned area at landscape and regional level. Our analysis first links observed gridded FWI data to annual burned area in the four landscapes. We then use - FWI projections from climate models to simulate future BA distributions under two emissions scenarios (RCP4.5 and RCP8.5) and two global climate models (HadGEM2-ES and CNRM-CM5). The BA distributions are incorporated in the REWILD-FIRE modelling framework to inform the REMAINS simulator of expected burned area in the simulation period (2018-2098). While FWI provides a useful indicator, it can be weak predictor of BA because it captures only the meteorological component of fire danger. BA is also influences by factors such as ignitions, fuel continuity and availability, suppression capacity and response time, topographic constraints, and strong non-linearities (e.g., thresholds, saturation, and years with severe fire weather but few ignitions or rapid containment). Many of these drivers are regional- or landscape-specific. Moreover, aggregating FWI to seasonal or annual means can smooth out the short-lived extremes that often dominate fire initiation and growth. To address these limitations, we aligned FWI predictors to the relevant fire season (October to March), derived seasonal metrics capturing both average conditions and extremes (peaks and upper quantiles), included landscape fixed effects to account for persistent site differences, and applied ridge regression to stabilize estimates under collinearity and weak signal. Finally, rather than reporting only

mean BA, we parameterized the full forecast distribution for 2025–2064, enabling support Monte Carlo sampling and explicitly represent variability and uncertainty.

This work is carried out in the following steps:

- Extract historical monthly FWI maps over each landscape and derive seasonal aggregated FWI predictors aligned with the fire season in Northern Italy (January-March and October-December).
- Quantify changes in mean level and variability of FWI mean and extreme metrics between historical and future periods.
- Calibrate an empirical BA model using observed historical aggregated FWI (1970–2021) and observed BA (2007–2024, overlapping years used), using landscape as a random factor.
- Apply the calibrated model to future monthly FWI projections to obtain annual BA simulations and compare BA distributions across periods.

FWI data was sourced from the '***Climate indicators for Europe from 1940 to 2100 derived from reanalysis and climate projections***' dataset provided by the Copernicus Emergency Management Service (CEMS; last updated January 2025). The dataset includes FWI from a historical re-analysis (1979 to 2021), based on the ERA5 reanalysis and produced for the Global ECMWF Fire Forecasting (GEFF) model and EFFIS, as well as projections from the *'Fire danger indicators for Europe from 1970 to 2098 – version 2.0'*. According to the data provider, simulations have daily temporal resolution and 0.1° spatial resolution, covering **RCP4.5 and RCP8.5** scenarios. We selected simulations from **HadGEM-ES (UK) and CNRM-CM5 (France)** to capture variability between climate models. herein this study, daily data were provided as **monthly aggregates at 0.25°** by the Copernicus. A **bias-correction procedure** adjusted the mean and variance of simulated FWI to match the reanalysis over the 1981–2010 reference period, ensuring statistical consistency between observed and simulated FWI, a key reason for choosing this dataset despite its coarser spatial and temporal resolution. Overall, 16 simulated scenarios were available (4 landscapes x 2 GCMs x 2 climate scenarios).

Landscape polygons were read from a shapefile, with the landscape identifier taken from the attribute 'layer'. For each NetCDF file, grid-cell values intersecting each polygon were extracted and **area-averaged**. FWI was aggregated to an annual 'fire-season relevant' value, using **months January-March and October-December** (, corresponding to the same solar year as the burned area data. From these, we derived seasonal predictors:

- fwi_mean_6mo: mean of monthly-mean FWI over the 6 fire-season months
- fwi_mean_peak: maximum monthly-mean FWI in the season
- fwi_max_peak: maximum of monthly-maximum FWI in the season.

Temporal trends in FWI were estimated separately for each landscape and for each scenario × GCM using ordinary least-squares regression of each annual metric against year. Changes in mean and variability (SD, IQR, and CV) were summarized for the historical reanalysis period (1970–2021) and two future windows (2025–2064 and 2065–2083). Observed BA (in ha) were aggregated from monthly to annual totals per landscape. The response variable was **log10(x) +1 transformed** to reduce heteroscedasticity and stabilize variance. We fitted a **ridge regression** (glmnet) using the three FWI predictors (fwi_mean_peak, fwi_mean_6mo, fwi_max_peak) and landscape fixed effects, with regularization strength selected via cross-validation. Predictions were back-transformed to hectares.

The calibrated model was then applied to projected FWI predictors for each landscape, scenario and GCM. To represent the *full range of plausible annual burned area (BA)* for 2025–2064, we parameterised the predicted annual BA distribution separately for each landscape × scenario × GCM combination (n = 40 years). A two-part (hurdle) structure was considered: (i) the probability of a zero-BA year (p_zero), and (ii) a continuous distribution for positive BA values (candidate families: lognormal and gamma, selected by AIC). For the 2025–2064, p_zero was 0 in all combinations (simulated BA was always positive after back-transformation), so the distribution was effectively continuous. Finally, predicted BA distributions were compared across periods (1985–2024, 2025–2064, and 2065–2083) and against observed distributions to assess model performance and projected changes.

2.1.2.1. Yearly burnt area distribution results

Across all calibration records (n=58 landscape-years), the ridge regression model accounted for moderate variance on the log scale (R^2=0.535, correlation=0.735; Table 3; Fig. 5 and 6).

Table 3. Performance by landscape (log scale)

Landscape	Years (n)	RMSE (log1p)	R^2 (log1p)	Corr (log1p)	RMSE (ha)
1A1B	15	1.5	0.394	0.683	718.8
1A2A	13	1.2	0.100	0.408	21.9
1A2B	15	1.4	0.147	0.395	121.9
1A2C	15	1.3	0.425	0.690	39.7

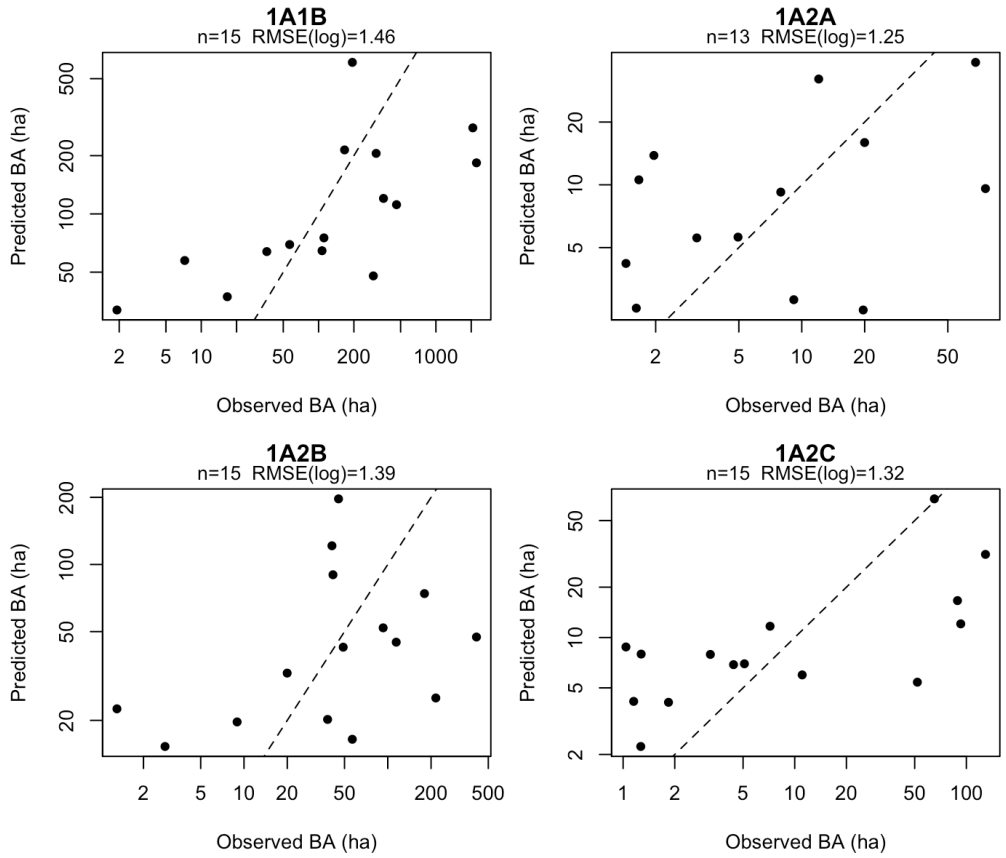

Figure 5. Observed vs predicted burned area (calibration period)

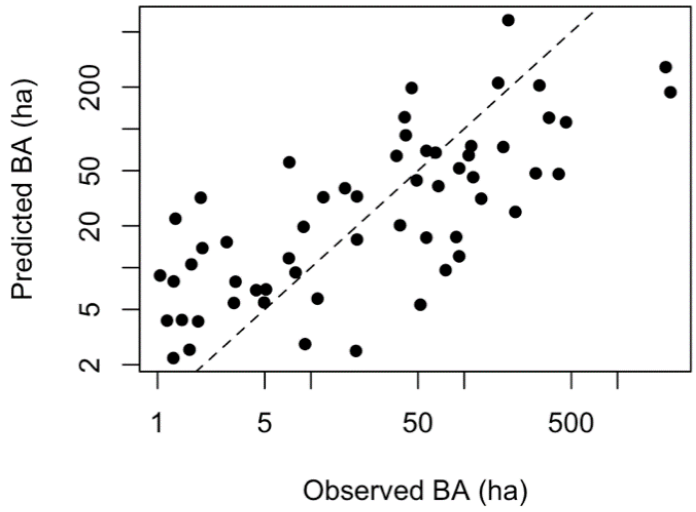

Figure 6. Observed vs predicted burned area (calibration period – all landscapes):

Changes were summarized for two representative indicators: fwi_mean_avg (the mean of monthly-mean FWI during the fire season) and fwi_max_p99 (the 99th percentile of monthly maxima during the fire season). These changes were compared between the simulated period (2018-2098) and the observed historical FWI (1970–2021) (Figure 7). All combinations of landscape x GCM x scenario showed **an increase in mean FWI and its standard** deviation, while changes in the coefficient of variation (CV) were not consistent.

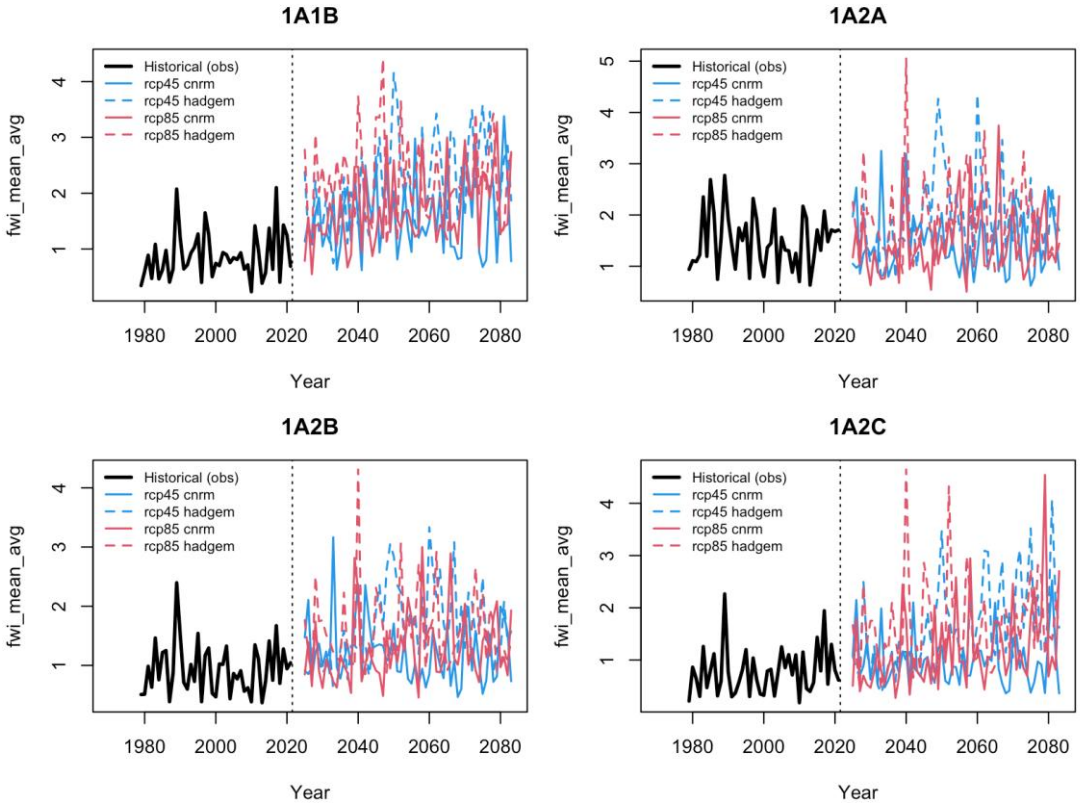

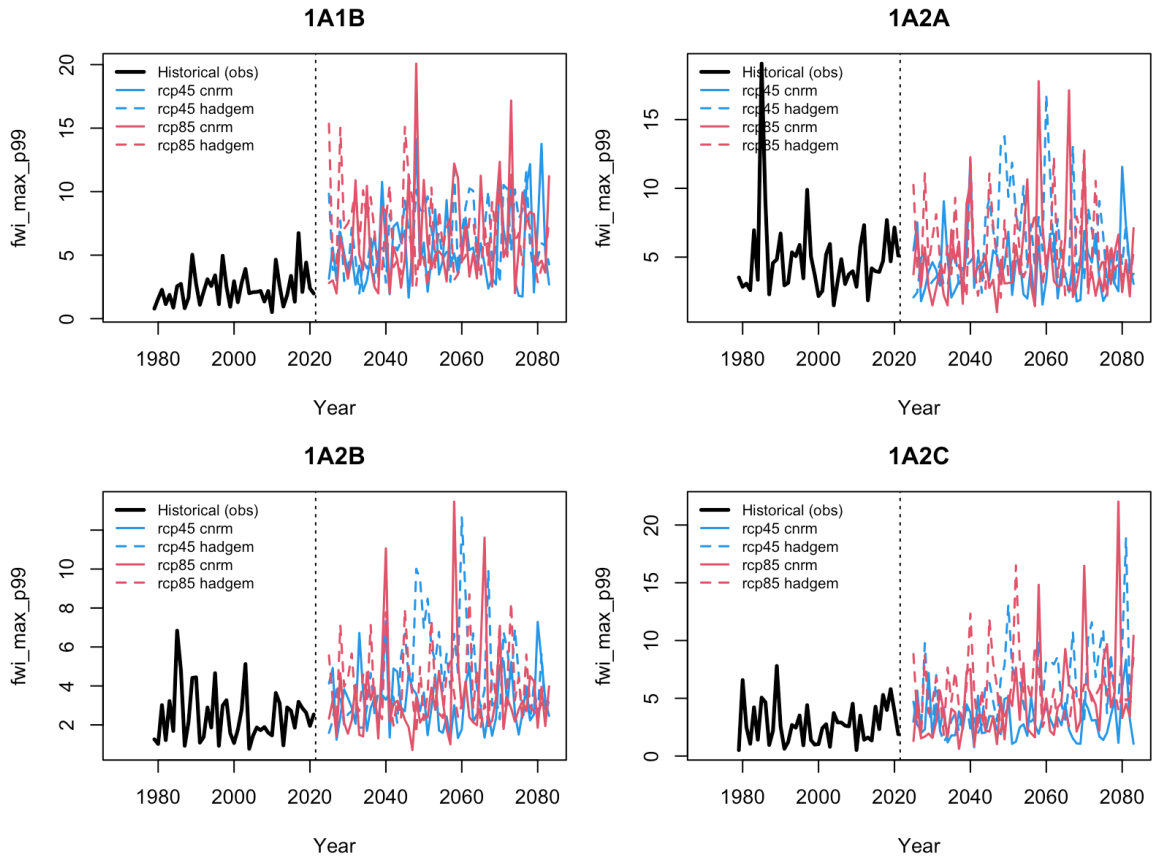

Figure 7. Temporal trend in observed and simulated FWI across four landscapes, for two climate scenarios (RCP4.5, RCP8.5) x two simulation sources (HadGEM-ES and CNRM-CM5). FWI mean (top 4 panels) and 99th percentile (lower 4 panels).

Applying the calibrated model to projected FWI resulted in markedly different BA distributions across GCMs and scenarios. The results were summarized using the mean, median, and upper quantiles of predicted annual BA (Table 4 and 5; Fig. 8 and 9). The HadGem GCM consistently predicted higher BA levels, while CNRM tended to maintain more stable distributions of BA over time. RCP 8.5 did not always produce higher or more variable burned area values than RCP 4.5.

Table 4. Median percent change relative to 1979-2021 (range across landscapes in parentheses)

period	metric	RCP	GCM	Mean change (%)	SD change (%)	CV change (%)
2025–2064	fwi_max_p99	rcp45	cnrm	19.4 (-10.6 to 122.7)	-4.7	-16.8
2025–2064	fwi_max_p99	rcp45	hadgem	87.2 (29.4 to 163.8)	72.3	-10.4
2025–2064	fwi_max_p99	rcp85	cnrm	32.1 (-3.5 to 147.5)	66.4	15.5
2025–2064	fwi_max_p99	rcp85	hadgem	86.1 (17.9 to 197.3)	59.8	-15.4
2025–2064	fwi_mean_avg	rcp45	cnrm	29.0 (-1.7 to 76.5)	15.9	-16.0
2025–2064	fwi_mean_avg	rcp45	hadgem	77.8 (27.9 to 132.5)	64.5	-8.2
2025–2064	fwi_mean_avg	rcp85	cnrm	30.4 (-4.6 to 76.6)	36.0	6.8
2025–2064	fwi_mean_avg	rcp85	hadgem	91.4 (29.6 to 150.6)	76.5	-2.9
2065–2083	fwi_max_p99	rcp45	cnrm	23.0 (-10.3 to 152.2)	16.8	-1.4
2065–2083	fwi_max_p99	rcp45	hadgem	119.5 (14.5 to 184.3)	79.4	-18.5
2065–2083	fwi_max_p99	rcp85	cnrm	101.1 (5.6 to 211.1)	131.6	15.4
2065–2083	fwi_max_p99	rcp85	hadgem	72.0 (2.6 to 168.6)	15.8	-20.5
2065–2083	fwi_mean_avg	rcp45	cnrm	26.5 (-4.3 to 91.6)	33.1	7.8
2065–2083	fwi_mean_avg	rcp45	hadgem	124.6 (25.9 to 183.0)	45.8	-29.1
2065–2083	fwi_mean_avg	rcp85	cnrm	76.1 (7.7 to 134.3)	49.5	-4.6
2065–2083	fwi_mean_avg	rcp85	hadgem	92.7 (12.1 to 153.1)	29.0	-34.4

Table 5. Summary statistics of predicted BA 2025-2064.

Landscape	RCP	GCM	period	Mean (ha)	Median (ha)	P90 (ha)	P99 (ha)
1A1B	rcp45	cnrm	2025–2064	196.7	120.5	407.8	1019.6
1A1B	rcp45	hadgem	2025–2064	1023.6	277.7	1183.7	13759.8
1A1B	rcp85	cnrm	2025–2064	168.1	110.9	391.7	920.9
1A1B	rcp85	hadgem	2025–2064	1881.7	266.8	1439.3	30681.0
1A2A	rcp45	cnrm	2025–2064	10.6	6.6	23.1	65.1
1A2A	rcp45	hadgem	2025–2064	45.9	11.8	58.0	573.2
1A2A	rcp85	cnrm	2025–2064	9.8	4.9	17.3	64.5
1A2A	rcp85	hadgem	2025–2064	124.8	11.8	88.8	2445.5
1A2B	rcp45	cnrm	2025–2064	118.9	47.9	181.1	1265.0
1A2B	rcp45	hadgem	2025–2064	201.9	91.6	623.3	846.0
1A2B	rcp85	cnrm	2025–2064	102.2	42.7	183.6	833.7
1A2B	rcp85	hadgem	2025–2064	662.5	83.6	476.7	12245.1
1A2C	rcp45	cnrm	2025–2064	15.6	9.4	18.0	89.7
1A2C	rcp45	hadgem	2025–2064	37.1	13.8	53.7	390.4
1A2C	rcp85	cnrm	2025–2064	18.4	7.0	56.1	110.0
1A2C	rcp85	hadgem	2025–2064	60.3	14.8	109.3	743.9

To account for the worst scenario, the yearly BA distribution predicted under the RCP8.5 - Hadgem scenario for each landscape was used for simulation analyses with the REMAINS model.

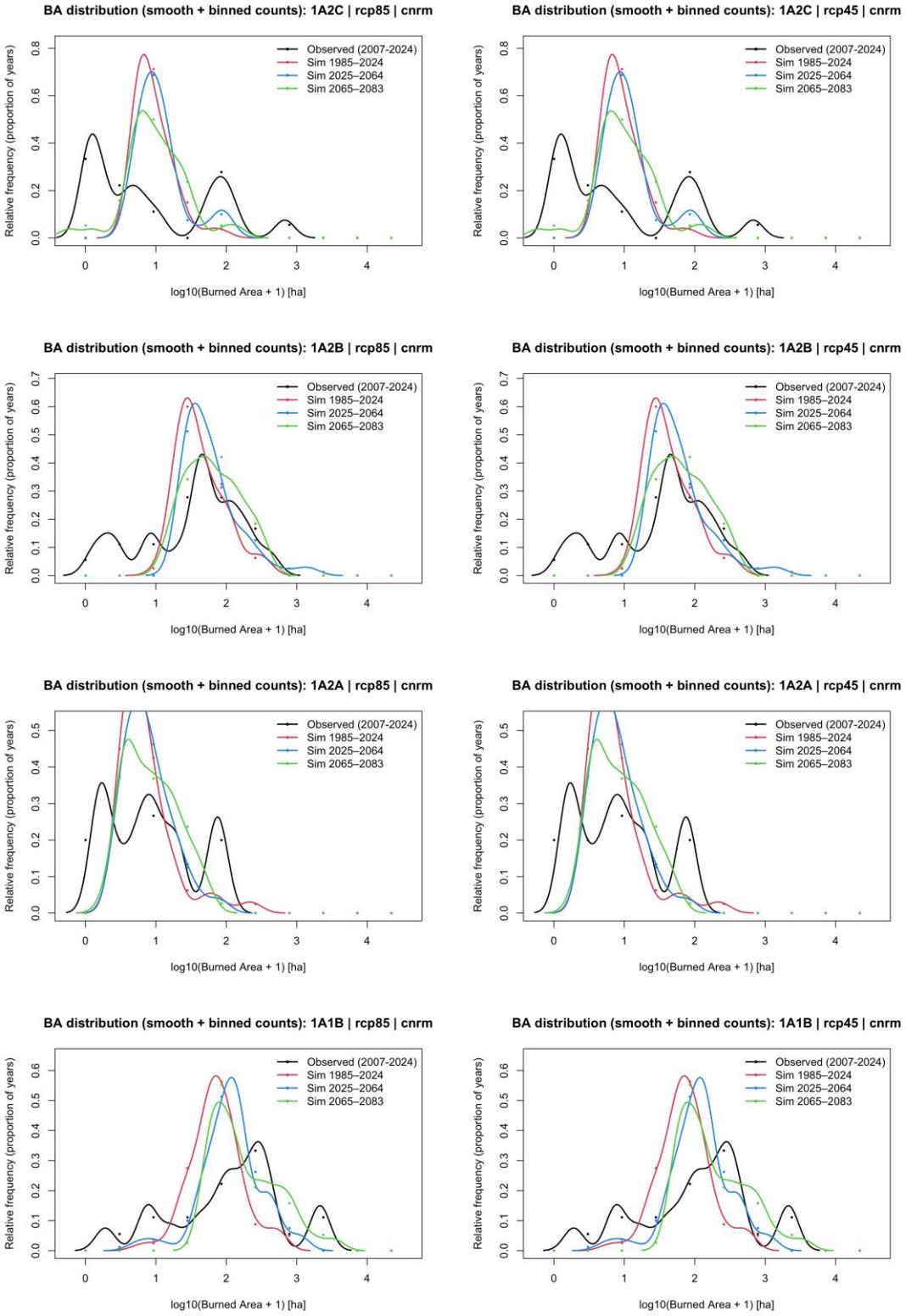

Figure 8. Distributions of BA in the observation window and three simulated periods (conditional mean, binned), for CNRM GCM

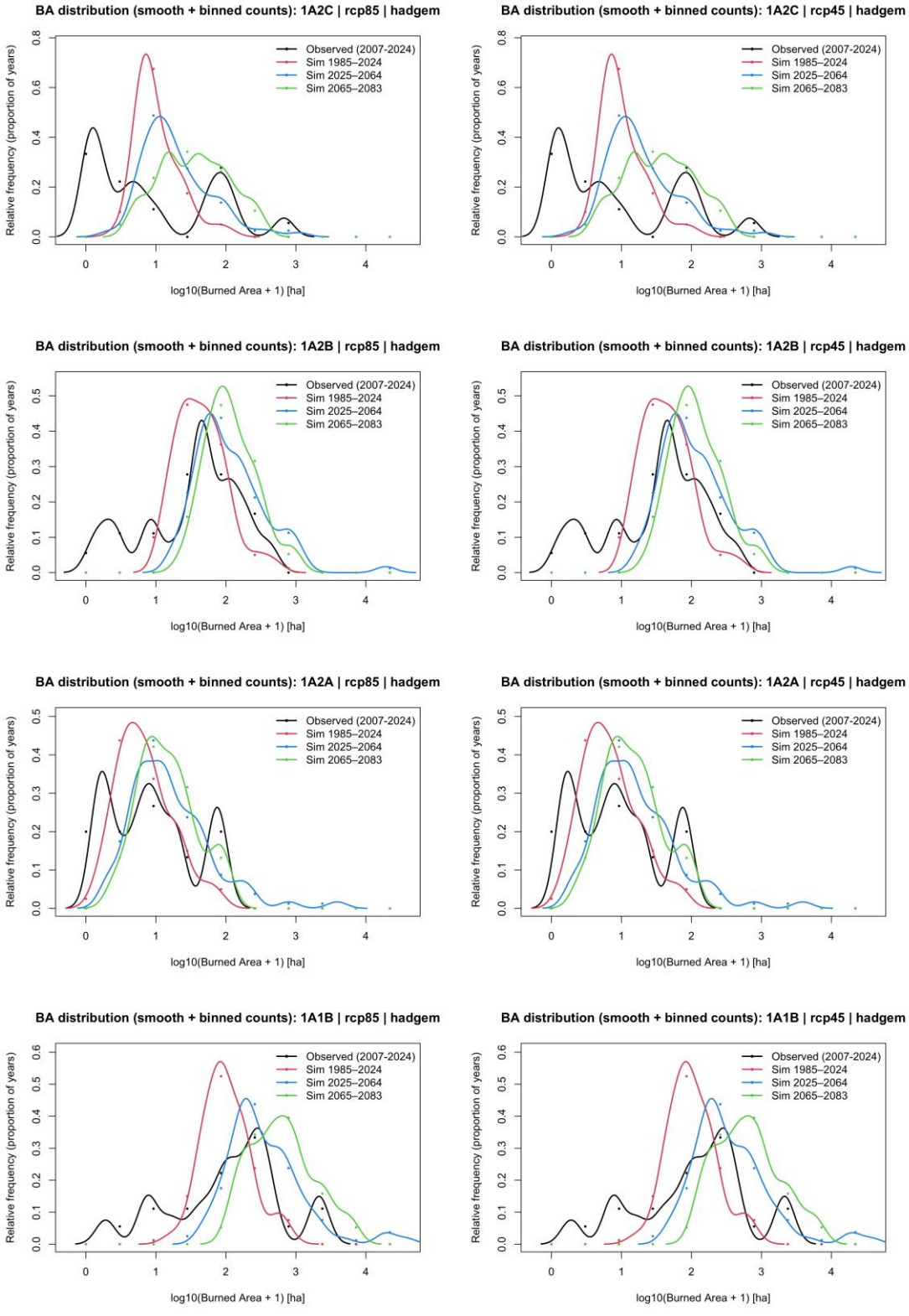

Figure 9. Distributions of BA in the observation window and three simulated periods (conditional mean, binned), with HadGem GCM

2.2. Fuel input data

2.2.1. Postfire transition matrix

A postfire transition matrix was generated by evaluating land cover type (LCT) transitions following fires of the 2007-2024 national dataset. LCT maps (Corine Land Cover - CLC) related to 2000 and 2018 were compared to assess these transitions. We did not differentiate among areas that were burned only once or multiple times. In the matrix, both columns and rows represent LCTs, with cell values indicating the proportion of each LCT that transitioned to another LCT during the period. A post-fire transition was assessed if a cell that experienced fire at any time during the study period had a different LCT in the 2007 and 2018 data sets. Post-fire transition matrices were produced for each ecoregion.

2.2.2. Flammability and fire susceptibility

We calculated a selectivity index for each LCTs burned by fires of the 2007-2024 dataset across the entire study area, defined as the ratio between LCT_n area burnt and total LCT_n area. This index was assumed to be proportional to the intrinsic flammability of each LCT. Based on this assumption, we derived a flammability vector, rescaled from 0 to 1.

Flammability vector: (urban = 0.00, crop = 0.20, pasture = 0.50, broadleaf = 0.71, conifer = 0.69, sparse = 0.76, shrub = 1.00, barren = 0.00, water = 0.00, shrub2con = 0.58, shrub2brd = 0.62)

This flammability vector can be modified by additional overlapping landscape features or processes. Moreover, it also varies with LCT age (Table 6). The resulting effective flammability, incorporating these modifications, is hereafter referred to as fire susceptibility.

Fire susceptibility was defined as follow:

- aging LCT (except broadleaf) = flammability vector * linear age class multiplier (1.4)
- aging LCT (broadleaf) = flammability vector * exponential age class multiplier
- managed LCTs = flammability vector - 0.3
- firebreaks = 0

Table 6. Flammability multiplicators per age class and land cover type

Age class	Multiplicator (all LCT except broadleaf)	Multiplicator (broadleaf)
new	1	0.6
6	2.4	0.8
12	3.8	1.15
18	5.2	2
28	6.6	2.5
64	8.0	3

So that:

$$Fire\ susceptibility_i = f(LCT_i, LCT\ age_i, management_i, firebreaks_i)$$

where i = 30x30 m landscape cell. While the variable of fire susceptibility variable was already implemented in REMAINS, its calculation through aging LCT, managed LCT, and firebreaks represents an innovation we introduced for the REWILDFIRE project. This approach was designed to capture the increase in flammability associated with greater available fuel loads in older vegetation (see Deliverable 2.1). Importantly, we distinguished broadleaf from all other flammable LCTs (crop, pasture, conifer, sparse, shrub, shrub2con, shrub2brd). For broadleaf forests, fire susceptibility was assumed to increase exponentially with age, reflecting surface biomass estimates from WP2 that showed an increase in deadwood and litter in aging stands (see Deliverable 2.1). In contrast, for all other flammable LCTs, fire susceptibility increased linearly with age. We also introduced a reduction of fire susceptibility in managed LCTs to represent the effect that active management has on fuel reduction (Spadoni et al., 2023, 2026). Finally, we assigned a null fire susceptibility to firebreaks, assuming such areas are continuously maintained and monitored to ensure very low levels of flammability and consequent efficiency in limiting fire spread (Ascoli et al., 2018).

2.3. Fire Risk sub-model

Within the 'fire.risk' model, fire ignitions are allocated probabilistically according to fire-risk layers. Fire risk is quantified at the cell level as the expected impact of a wildfire, defined by the combination of fire hazard and potential damage.

$$Fire\ Risk_i = Fire\ Hazard_i * Potential\ Damage_i$$

where i = 30x30 m landscape cell.

Fire hazard represents the likelihood and potential intensity of fire spread and is computed as the product of an ignition probability layer, a topographic multiplier derived from slope, and fire susceptibility. As explained above (section 2.2), fire susceptibility reflects vegetation flammability and fuel structure, incorporating baseline flammability values by land-cover type (LCT), age-dependent modifiers (notably differing between broadleaf and conifer forests), and reductions associated with management actions; it is set to zero in non-burnable areas such as firebreaks.

$$Fire\ Hazard_i = Ignition\ probability_i * Topographic\ factor_i * Fire\ susceptibility_i$$

where:

- i = 30x30 m landscape cell
- Ignition probability$_i$ =
- Topographic factor$_i$ = multiplier given per slope classes
- *Fire susceptibility$_i$ = defined in section 2.1.*

Potential damage is estimated as the product of land-cover-type specific vulnerability coefficients and the economic or ecological value assigned per unit area, also assessed for each LCT.

$$Potential\ Damage_{LCT} = vulnerability_{LCT} * value_{LCT}$$

where LCT = Land Cover Type

Overall fire risk thus emerges as the interaction between the probability and capacity extent of fire spread and the expected losses if fire occurs, explicitly linking ignition likelihood, landscape properties, vegetation characteristics and exposure of valued assets within a spatially explicit framework. Within the REWILDFIRE project, we reviewed and updated LCT vulnerability and value

coefficients to reflect the social-ecological context of the alpine region and our specific landscapes. Since firebreaks were assigned zero fire susceptibility, the resulting fire risk was also zero in these areas.

2.3.1. Fire Risk maps

With the fire risk sub model, we were able to calculate the fire risk variable and spatialise it to produce fire risk maps (Fig. 10-13). The analysis clearly revealed a gradient of fire risk among landscapes with the 1A1b showing the highest values.

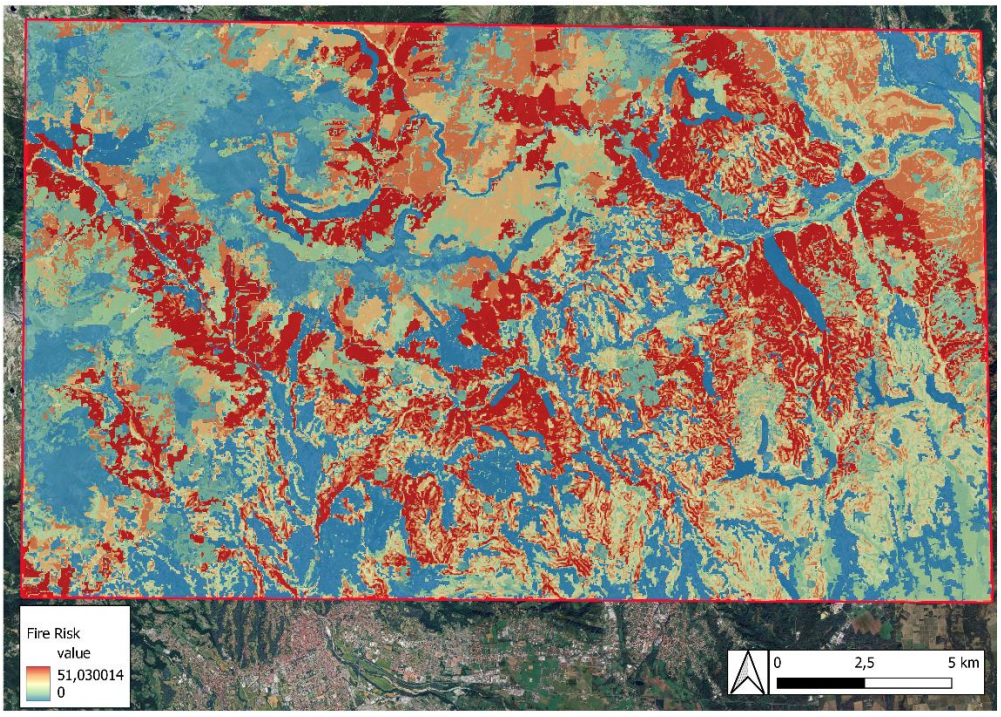

Figure 10. Fire risk map at simulation year 5 for the landscape 1A1b

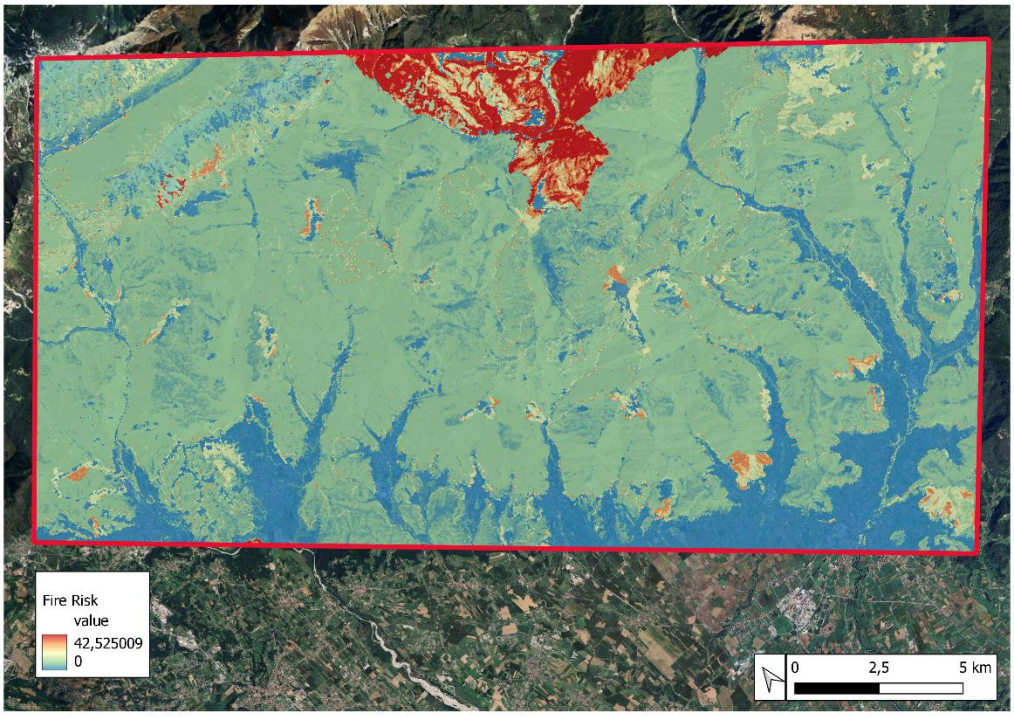

Figure 11. Fire risk map for the landscape 1A2a

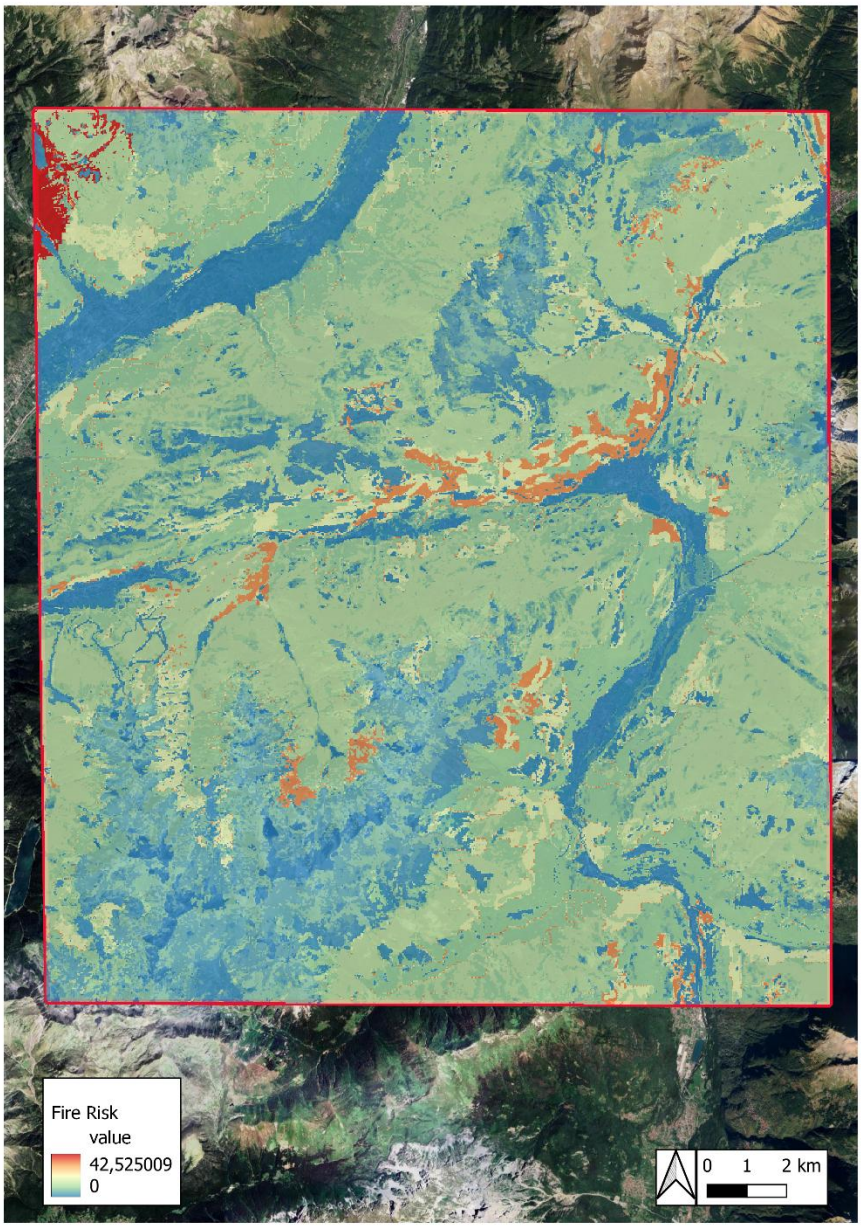

Figure 12. Fire risk map for the landscape 1A2c

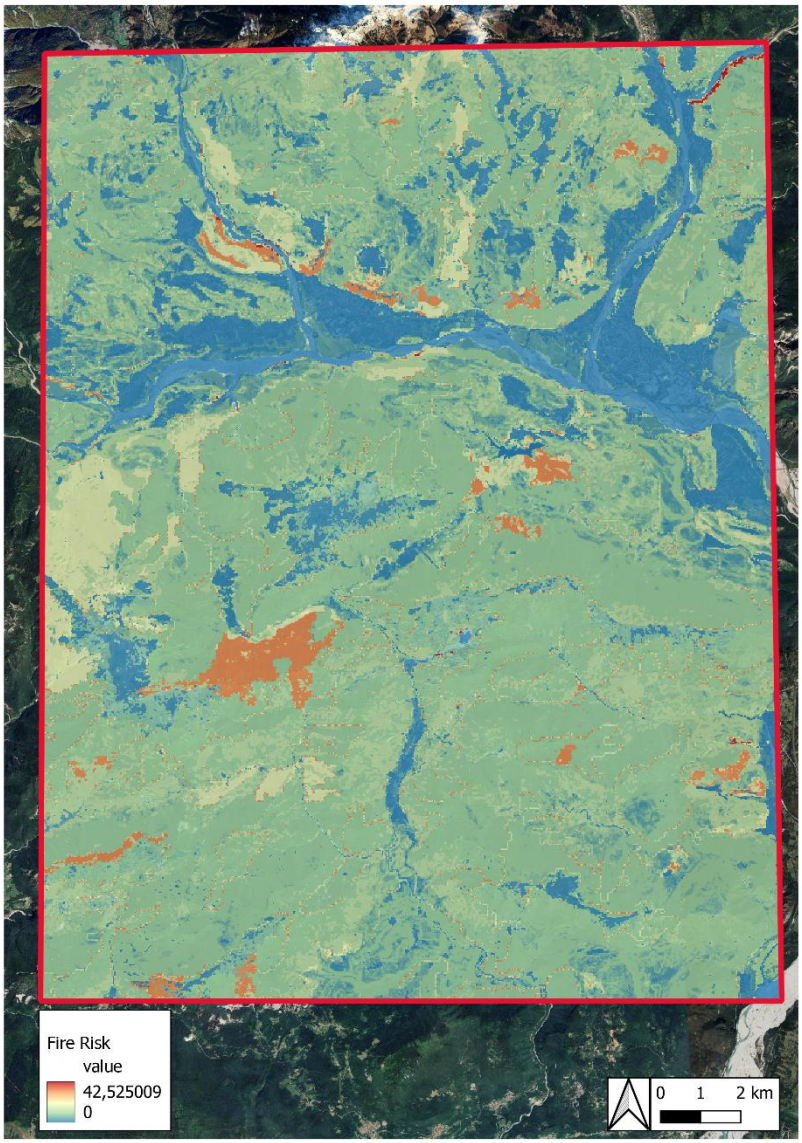

Figure 13. Fire risk map for the landscape 1A2b

2.4. Wildfire sub-model

2.4.1. Annual target burned area and fire events.

In this sub-model, wildfire spread is simulated on annual basis. At each simulated year, the model first selects an annual target burned area (ha), by sampling from the input data of burned area distribution, representing the area potentially affected by fire during that year. If the annual target area is zero, no wildfires are simulated for that year, although this condition did not occur in our simulations as we excluded years with zero fires from the selection. The annual target area is then progressively consumed by a sequence of individual fire events. For each fire event, a fire-specific target area is sampled from the input data of fire-size distribution and constrained so that it does not exceed the remaining annual target area. Fire events are simulated sequentially until the annual target area is exhausted or no further spread is possible.

$$Annual\ target\ burned\ area_{\ year\ i} = \sum_{j=1-n} fire\text{-}specific\ target\ area_{\ year\ i;\ fire\ j}$$

However, fire-specific target area is a potential measure, and it does not represent effectively burned area as it also includes suppressed area. Mechanisms of fire suppression are detailed in the following section 2.4.

$$fire\text{-}specific\ target\ area_{\ year\ i;\ fire\ j} = effectively\ burnt\ area_{\ year\ i;\ fire\ j} + suppressed\ area_{\ year\ i;\ fire\ j}$$

The variables of annual target burned area and the single fire-specific target area, randomly drawn from the burned area and fire size distributions, introduce a stochastic component to the model, which is further amplified by the spatial distribution of ignition location and landscape configuration.

2.4.2. Fire events ignition and spread.

Each fire event begins from a single ignition cell, selected probabilistically according to fire-risk values assessed within the fire-risk sub-model. According to the definition of fire-risk, ignitions can occur only in flammable LCTs and outside firebreaks.

Fire spread is simulated using an eight-neighbour (queen's case) approach on the 30x30m raster grid. At each spreading step, candidate neighbouring cells are evaluated and assigned a spread-rate parameter (SR), which represents the relative potential for fire propagation from an active burning cell to a target cell. SR is defined as a linear combination of slope effects and fire susceptibility.

$$SR_i = slope_i * w_{slope} + fire\ susceptibility_i * w_{LCT}$$

Where:

- i = 30x30 m neighbouring cell
- Slope = is a normalized slope term derived from elevation differences between source and target cells, ranging [0,1];
- *Fire susceptibility$_i$ = defined in section 2.1.*
- w_{slope} and w_{LCT} are weighting parameters controlling the relative influence of topography and fuels; respectively equals to 0,35 and 0,65.
- SR can vary among [0; 2,30]

For each evaluated neighbour cell, SR is translated into a **probability of burning** (p_b) using an exponential function.

$$P_{b\ i} = 1 - \exp(-f_{acc} * SR_i) + \varepsilon$$

Where:

- i = 30x30 m neighbouring cell
- f_{acc} = is a fire-acceleration parameter equal to 3.
- ε = is a stochastic term, extracted by a uniform distribution centred on zero and bounded between [-0,2; 0,2], that introduces local variability in fire patterns

Then, a cell is affected by the fire front when P_b exceeds a random threshold, $P_{b\ threshold}$, which is drawn from another uniform distribution bounded between [-0,8;1].

$P_b >= P_{b\ threshold}$ *:* neighbour cell is affected by the fire front

$P_b < P_{b\ threshold}$ *:* neighbour cell is not affected by the fire front

This formulation, which includes two stochastic filters (ε and $P_{b\ threshold}$), ensures stochastic fire shapes. With ε, cells with moderate or low SR may still burn occasionally, and cells with high SR may occasionally fail to burn, leading to more irregular and realistic fire perimeters. Conceptually ε represents small fuel discontinuities and micro-topographic effects that do not alter large-scale fire directionality but increases the realism of local fire spread. Instead, the variable threshold $P_{b\ threshold}$ represents randomness of burning due to other unobserved factors (e.g., linked to suppression decisions or combustion dynamics).

Neighbouring cells that satisfy the condition imposed on the probability of burning become part of the active fire front. Fire fronts may consist of multiple cells, with their size depending on fire-specific target area, spreading phase, and stochastic sampling to avoid unrealistically compact or overly fragmented perimeters. In particular: larger fires are associated with larger fire fronts; fire fronts are small at early phases of the fire event; they get the largest fire front size at intermediate phases and recontract again in the late phases. Spreading phases are identified by the ratio given by the sum of burnt and suppressed areas over the fire-specific target area.

Fire spread continues iteratively until one of the following conditions is met: (1) the fire-specific target area is reached (including burned and suppressed cells); (2) no additional cells can be activated from the current fire front.

2.5. Fire Suppression Mechanisms

Fire suppression is simulated through three complementary mechanisms, applied at the cell level: (1) Fuel suppression, (2) Mosaic suppression, and (3) Firebreak suppression. While the first two were already present in the original REMAINS model by Duane et al. (2016), the latter was an innovation we introduced for the REWILDFIRE project. We also imposed that these three components equally account to the total suppressed area. Candidate cells for the advancement of the fire front and that meet the conditions to be suppressed by one of these mechanisms, are accounted as suppressed areas.

So that:

$$suppressed\ area_{\ year\ i;\ fire\ j} = fuel\ suppressed\ area_{\ year\ i;\ fire\ j} + mosaic\ suppressed\ area_{\ year\ i;\ fire\ j} + firebreak\ suppressed\ area_{\ year\ i;\ fire\ j}$$

Firebreak suppression has priority over other suppression mechanisms, and mosaic suppression has priority over fuel suppression.

2.5.1. Fuel suppression

Cells are suppressed when their spread-rate parameter (SR) falls below a predefined threshold ‘fuel.th’. Cells with a SR lower than ‘fuel.th’ represent low-intensity fire behaviour that can be effectively controlled by firefighting efforts. As it will be introduced in the next sections (3.2), we set two different fuel.th according to the simulations’ scenarios: the scenario ‘StR_S’, where we simulated increased suppression effort, had an increased fuel.th (0.4), compared to the other scenarios (0.3).

2.5.2. Mosaic suppression

Fires are suppressed when the fire front encounters sufficient agricultural continuity, expressed as a minimum number of consecutive crop cells, mimicking suppression opportunities created by landscape heterogeneity. This works for fire fronts of any size. The mosaic threshold ‘mosaic.th’ was

set equal to 2 cells for all the scenarios, i.e., nearly 2000 m^2, as it will be shown in section 3.2. We set a low threshold to enhance the agricultural mosaic effect within our simulations.

2.5.3. Firebreak suppression

Cells designated as firebreaks cannot burn and immediately suppress fire spread when encountered. This type of suppression was introduced as an innovative tool in this version of REMAINS, and present only in the scenarios that involve direct fire prevention through firebreaks.

2.6. Fire Effects

The passage of fire on the landscape can have multiple effects.

- **Land cover change**: based on the probabilities in the post-fire transition matrix, fire can lead to a change in land cover type (LCT). When this occurs, the new post-fire LCT restarts aging from zero.
- **Forest rejuvenation** (non-stand-replacing fires): for forest cells (broadleaf and conifer), if the post-fire LCT remains the same (broadleaf → broadleaf; conifer → conifer), fire reduces the age of burned cells to the previous age class. This rejuvenation mechanism represents the effect of fuel reduction caused by fire. Renewed forest thus has lower flammability and reduced carbon storage, both of which depend on LCT age. Fires triggering this process are referred to as non-stand-replacing fires (Table 7). This rule applies only to forest cells, not to other LCTs.
- **Stand-replacing fires**: within the forest rejuvenation mechanism, if burned cells are first-age-class forests (broadleaf or conifer), they do not revert to age zero. Instead, they undergo land cover change, remaining for four simulation years within the transitional classes 'shrub-to-broadleaf' or 'shrub-to-conifer'. Fires triggering this process are classified as stand-replacing fires. Any residual areas of these transitional classes at the end of the simulation are assigned age zero to simplify the evaluation of carbon dynamics.

Table 7. Age classes for forest land and the effects of non-LCT-transitioning fires.

Initial age classes (years)	non-LCT-transitioning fires' effect on age class (-)
< 6	transition to 'shrub-to-broad' and 'shrub-to-con' classes and permanence for 4 years
6 – 12	shift to <6
12 – 18	shift to 6 – 12
18 – 28	shift to 12 – 18
28 – 64	shift to 18 – 28
> 64	shift to 28 – 64

2.7. Fire management strategies

Strategies for fire management were simulated as: fire suppression, direct prevention through firebreaks, and indirect prevention through the expansion of the agricultural mosaic. The implementation of direct and indirect prevention was innovative with this updated version of REMAINS developed for the REWILDFIRE project.

2.7.1. Fire suppression strategies

Fire suppression, simulated through the mechanisms described in section 2.5, represents the potential to stop fire spread through firefighting (fuel suppression) and through the agricultural mosaic (mosaic suppression). We also attributed a suppression potential to firebreaks to reflect improved firefighting accessibility.

2.7.2. Direct fire prevention (firebreaks)

Direct fire prevention was associated with the implementation of firebreaks over around 2% of the surface of each landscape, corresponding to approximately 800/850 hectares across landscapes. To represent real conditions, firebreaks were located within 50 m buffers from the road network (all viability including forest roads), and so to intercept most of the historic fires from the 2007-2024 national dataset (Figure 14). Firebreaks were built over flammable LCTs only.

Firebreaks did not imply any LCC, but they shifted back the covered surface by one age class. As described in section 2.2.2, firebreaks were associated with a null fire susceptibility, so that they could not burn, with the assumption that these infrastructures were constantly monitored and maintained to have a minimal fuel load. However, as explained in section 2.4, candidate burnable firebreaks cells were treated as areas where fire suppression occurs, representing the effects of firebreaks on limiting fire spread.

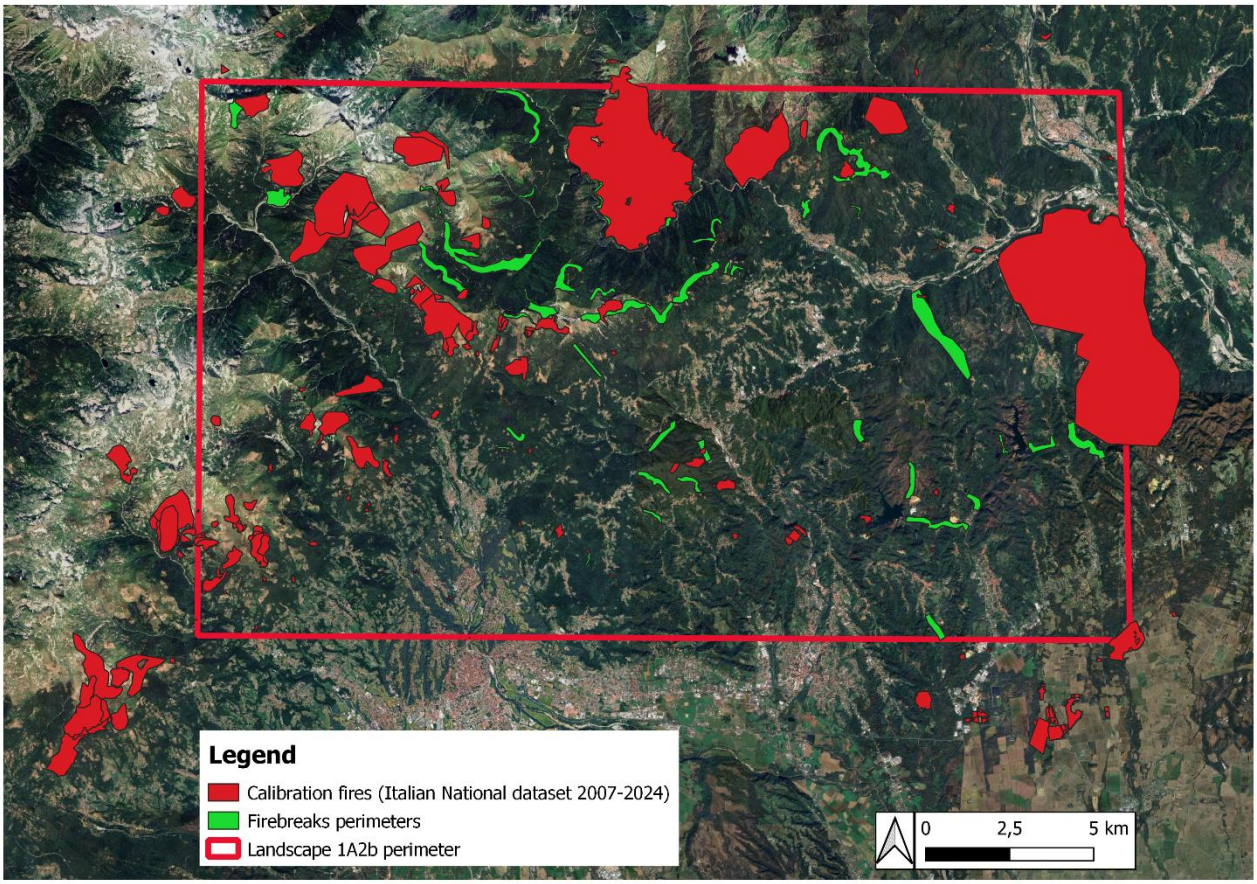

Figure 14. firebreaks and fire perimeters from the 2007-2024 Italian national dataset. Landscape 1A1b.

2.7.3. Indirect fire prevention (enhanced agricultural mosaic)

Indirect fire prevention was simulated as an expansion of the agricultural mosaic, consistent with literature indicating that landscape discontinuities, including LCTs with reduced fuel loads such as crops, can limit both fire ignition and spread (Spadoni et al., 2023).

To simulate indirect prevention, we modified the input landscapes by converting portions of forest cover into crops. Specifically, we transformed 5% of broadleaf cover and 5% of conifer cover into crops, selecting among forests younger than 18 years. Along with these conditions, we also chose to set new crops within blocks of at least 15 pixels and within successive 150 m buffers from firebreaks. For instance, if selected percentages were not reached within 150 m buffers, then 300 m buffers could be used. Indirect prevention was realised with these rules mimicking outcomes from rural development strategies to retake recently abandoned crops, giving priority to those areas that, combined with firebreaks, can contribute to shaping a fire resistant and resilient landscape. The suppression mechanism associated with the expanded crop surface worked as explained in section 2.5.

3. Land use scenarios

3.1. Landscape management strategies

Before presenting the simulated scenarios, it is useful to describe the landscape management strategies defined within REWILDFIRE. We implemented two landscape management strategies, which, in combination with fire management strategies (section 2.7), formed the basis for our simulation scenarios.

❖ **Active land management**

Active land management in the model halted aging in the LCTs to which it was applied, specifically broadleaf, conifer, pasture, and crop. In addition, managed areas were not affected by land cover changes (LCC) as modelled by lcc.demand, except through the passage of fire and according to the postfire transition matrix. While these areas remain burnable, their age is frozen, resulting in reduced fire susceptibility, which is further decreased by a coefficient of −0.3. Managed forest areas were distributed within 150 m successive buffers along forest viability, while managed pastures were located randomly but grouped into paddocks with a surface equal to total pasture surface divided by 50, and a minimum surface of one pixel. Crops were considered fully managed across all scenarios. This set of conditions aimed to represent active landscape management and its positive effect of fuel reduction under realistic conditions of accessibility (Spadoni et al., 2023, 2026).

❖ **Rewilding**

Rewilding was defined as a passive landscape management strategy aimed at allowing vegetation to develop according to its natural dynamics, without any form of intervention (Spadoni et al., 2026). According to this definition, within REWILD-FIRE, rewilding was meant as a process opposed to active land management, where areas under rewilding undergo unitary aging, meaning that each simulation year corresponds to one year of vegetation aging (‘unitary aging’).

Rewilding differs from simple absence of management, which also follows unitary aging but lacks intentionality. In line with the EU Biodiversity and Forest strategies, 10% of land surface of each EU country should not be subject to active interventions, assuming that rewilding leads to positive

outcomes in terms of ecosystem services, including carbon stock. Accordingly, in REWILD-FIRE we set a target of 10% of each landscape's surface under rewilding, selecting areas from all LCTs except urban, water, barren, and cropland.

Because unitary aging under rewilding can potentially increase fire impacts, we defined rules for locating rewilding areas that optimize trade-offs between ecosystem benefits, fire risk, and local bioeconomy potential. In particular, we distinguished two types of rewilding: 'strict rewilding' and 'fire-smart rewilding'.

The **strict rewilding** area was divided into the following three sequential pools, which were filled, one after the other, with each pool being completed before moving on to the next.

- 'Rw' pool: rewilding areas were established within unmanaged areas inside protected areas.
- 'Rwm' pool: if not possible to reach 10% of the landscape under rewilding with 'Rw', additional rewilding areas were placed within managed areas inside protected areas.
- 'Rwu' pool: if 'Rw' and 'Rwm' were saturated, additional rewilding areas were placed unmanaged areas outside protected areas, though within successive 1 Km buffers from protected areas.

Indeed, in line with European strategies, our hypothesis relies on the use of Protected Areas for spontaneous vegetation dynamics, while carefully considering the trade-offs discussed above.

The **fire-smart rewilding** followed the same procedure as strict rewilding, with the additional rule that Rwm could not be placed on pixels with an unmanaged flammability value trespassing the threshold equal to: 0.7. This strategy complemented strict rewilding with an inclusion of fire risk mitigation. All strategies were implemented differently across Land Cover Types (Table 8).

Table 8. LCTs and associated processes and strategies

LCT	**process / strategy**			
	fire (burnable LCTs)	firebreaks	landscape management	rewilding
urban	NO	NO	NO	NO
crop	YES	YES	YES	NO
pasture	YES	YES	YES	YES
broadleaf	YES	YES	YES	YES
conifer	YES	YES	YES	YES
sparse	YES	YES	NO	YES
shrub	YES	YES	NO	YES
barren	NO	NO	NO	NO
water	NO	NO	NO	NO

3.2. Simulated scenarios.

We simulated four different scenarios within REMAINS: 'Business as usual' (BAU), 'Strict Rewilding and Suppression' (StR_S), 'Fire Smart Rewilding and Direct Prevention' (FSR_DP), 'Fire Smart Rewilding and Direct and Indirect Prevention' (FSR_DIP; Fig. 15).

- BAU acted as a control scenario, in which no fire management, nor rewilding strategies were implemented. Landscape management and suppression levels were set at their standard levels.

- In StR_S we introduced strict rewilding and increased suppression (fuel suppression). This scenario represents policy choices that do not take into account fire behaviour and ecology. Indeed, our hypothesis is that investing in fire suppression contributes to creating the so-called 'fire-fighting trap', as it leads to fuel accumulation and subsequent larger and more intense fires. And also, that locating rewilding without accounting for fire risk can exacerbate impacts from fires.
- FSR_DP adopts fire-smart rewilding, introduces direct fire prevention, and retakes suppression levels to those of BAU. This scenario reflects investments targeting both fire prevention through green infrastructures (firebreaks) and overall fire-risk mitigation.
- FSR_DIP, as FSR_DP, involves planning rewilding in areas with low fire hazard ("fire-smart rewilding"), strategically implementing preventive infrastructure, e.g., fuel breaks to protect these rewilding zones, and combining direct fire prevention with investments in the agromosaic (agriculture and forestry management), which indirectly help mitigate fire activity. Table 9 resumes the scenarios' conditions.

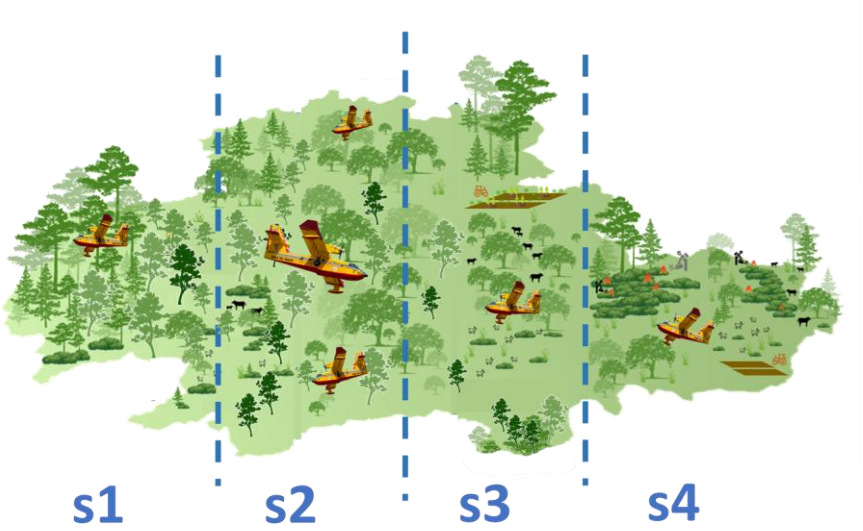

Figure 15. Scenarios representation: s1 – BAU; s2 – StR_S; s3 - FSR_DP; s4 – FRS_DIP. Conditions represented in each scenario are listed in Table 9.

Table 9. Simulated scenarios with associated strategies.

Scenario	**Fire management strategies**					**Landscape management strategies**				
	Suppression			Prevention		Landscape management*			Rewilding	
	fuel (-)	mosaic (cells)	firebreak	direct	indirect	forest (%)	pasture (%)	crop (%)	strict	fire-smart
BAU	0.4	2	NO	NO	NO	30	20	100	NO	NO
StR_S	0.75	2	NO	NO	NO	30	20	100	YES	NO
FSR_DP	0.4	2	YES	YES	NO	30	20	100	NO	YES
FSR_DIP	0.4	2	YES	YES	YES	40	20	100	NO	YES

* values refer to initial managed surface, without accounting for management area that is withdrawn due to rewilding (Rwm)

4. Results

4.1. Burned and Suppressed Areas

4.1.1. Total burned area patterns.

Trends in total burned area across the four landscapes (Figure 16-19) exhibit heterogeneous patterns. In landscape 1A1b, the most flammable case study, scenarios with direct (FSR_DP) and indirect (FSR_DIP) prevention consistently reduce burned area throughout the simulation period. Among these, FSR_DIP yields the lowest overall burned area, while FSR_DP shows the lowest variance around its mean (Figure 16). In the other landscapes, differences among scenarios are less pronounced. However, particularly towards the end of the period, both FSR_DP and FSR_DIP tend to maintain lower burned areas values compared to BAU (Figure 17-19).

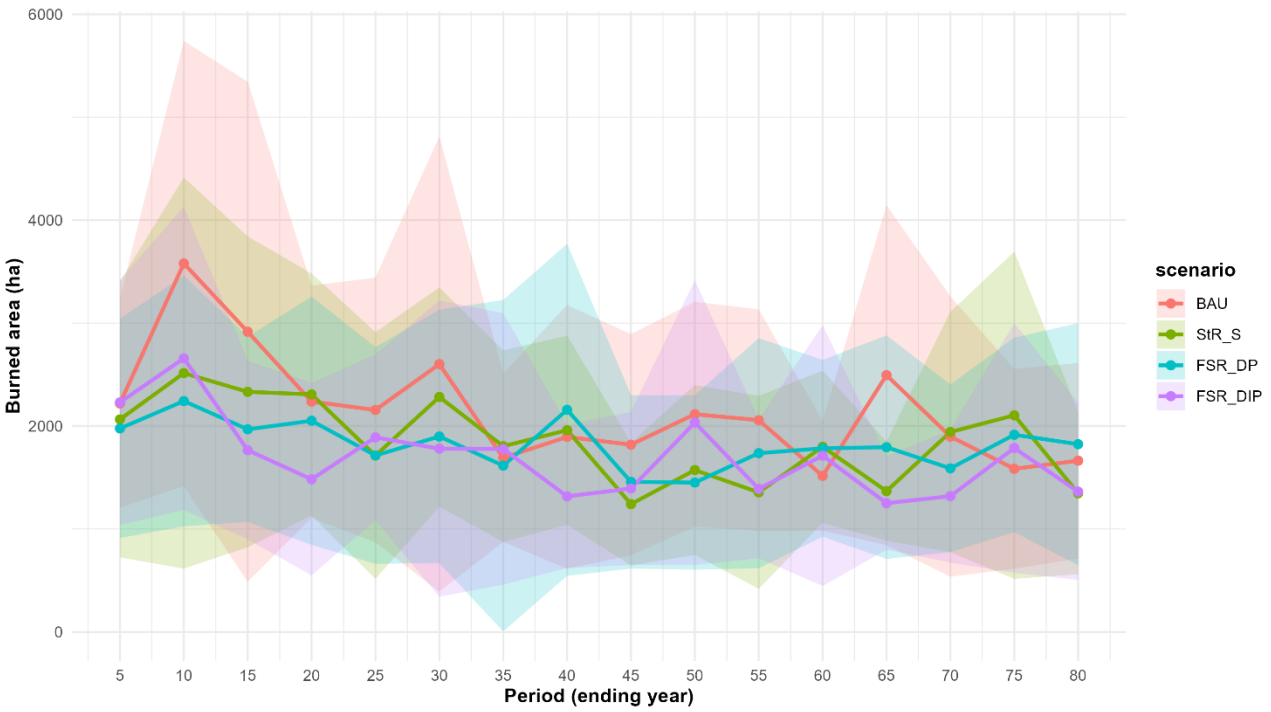

Figure 16. Total burned area (5-years totals; mean ± sd across runs: replicates for each scenario). Each point represents the sum of burned area in the previous 5 years. Results for the landscape: 1A1b

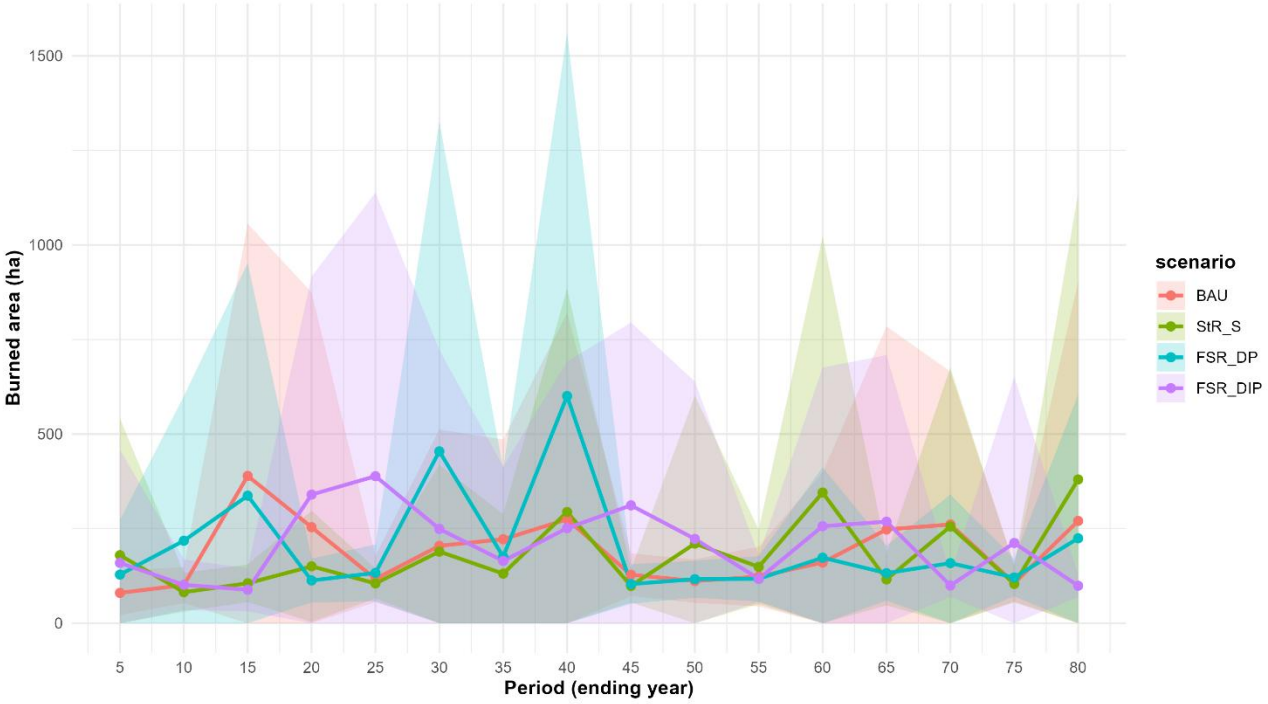

Figure 17. Total burned area (5-years totals; mean ± sd across runs: replicates for each scenario). Each point represents the sum of burned area in the previous 5 years. Results for the landscape: 1A2a

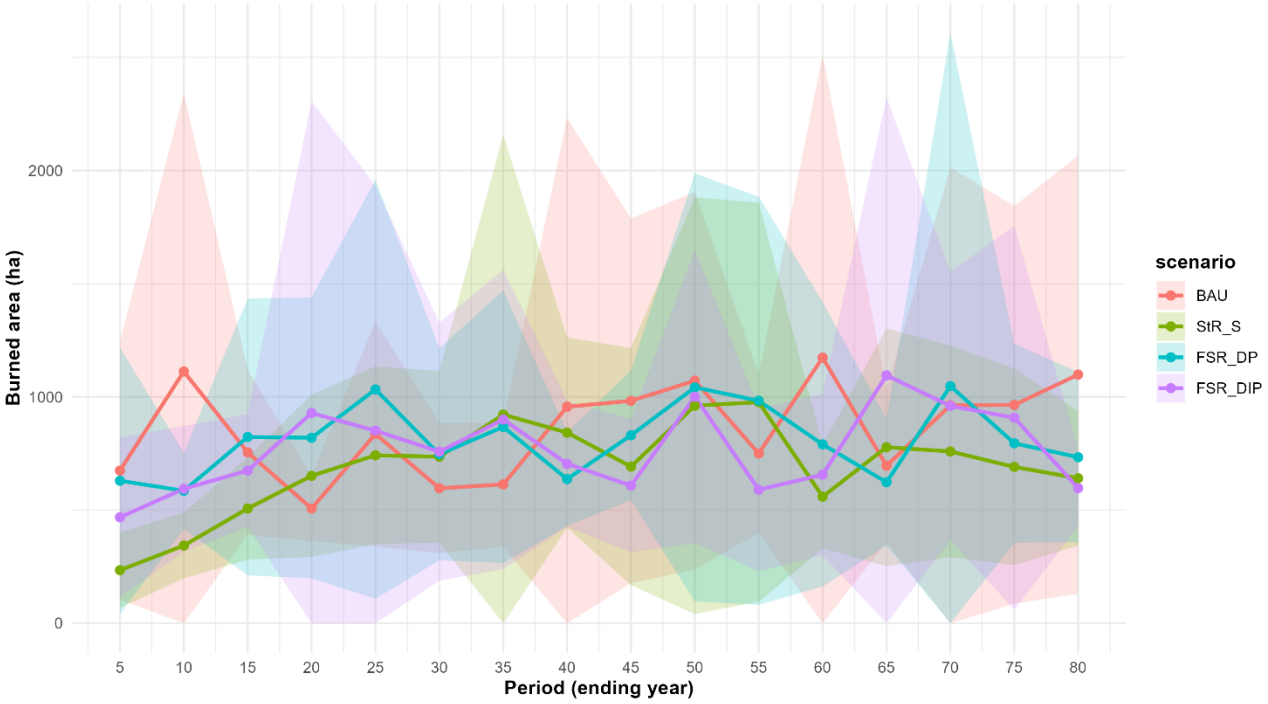

Figure 18. Total burned area (5-years totals; mean ± sd across runs: replicates for each scenario). Each point represents the sum of burned area in the previous 5 years. Results for the landscape: 1A2b

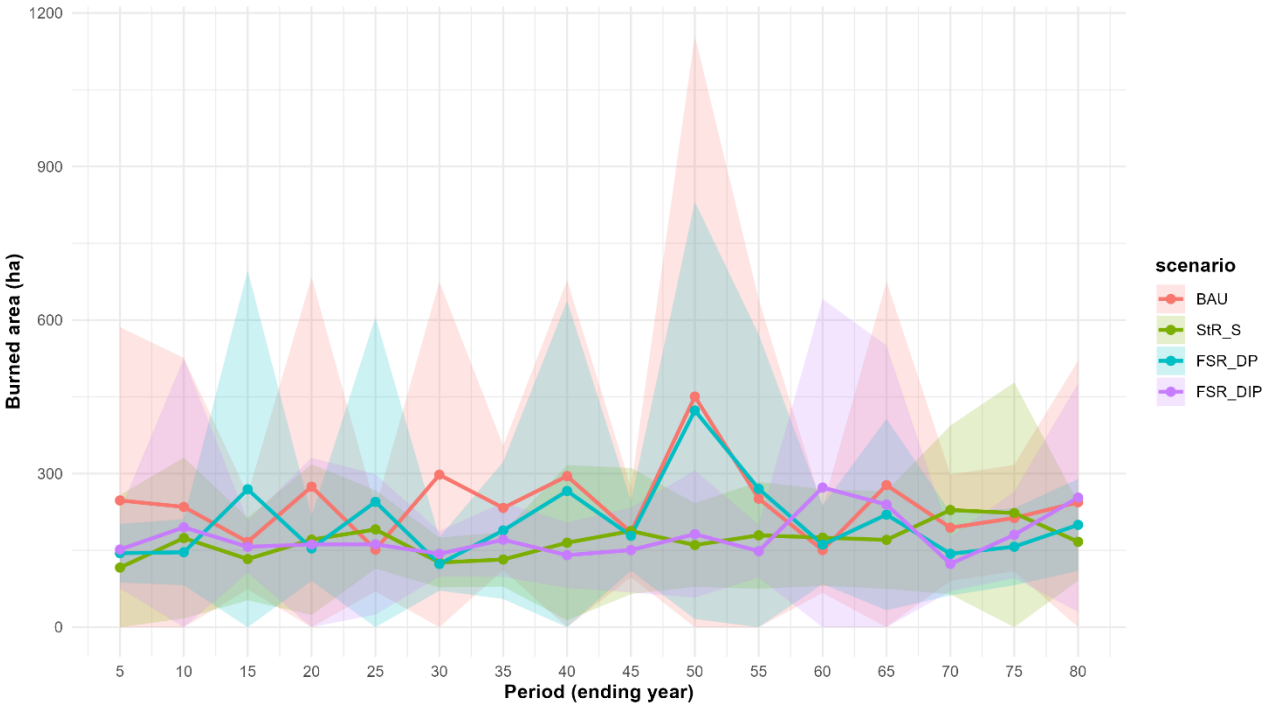

Figure 19. Total burned area (5-years totals; mean ± sd across runs: replicates for each scenario). Each point represents the sum of burned area in the previous 5 years. Results for the landscape: 1A2c

4.1.2. Total suppressed area patterns

StR_S and FSR_DIP show the highest values of suppressed area across landscapes, as these scenarios combine increase suppression efforts in terms of response (fuel suppression) with the enhancement of the agromosaic (mosaic suppression). However, FSR_DP exhibits the highest suppression peaks specifically in landscapes 1A2a, 1A2b, and 1A2c (Figure 21-23).

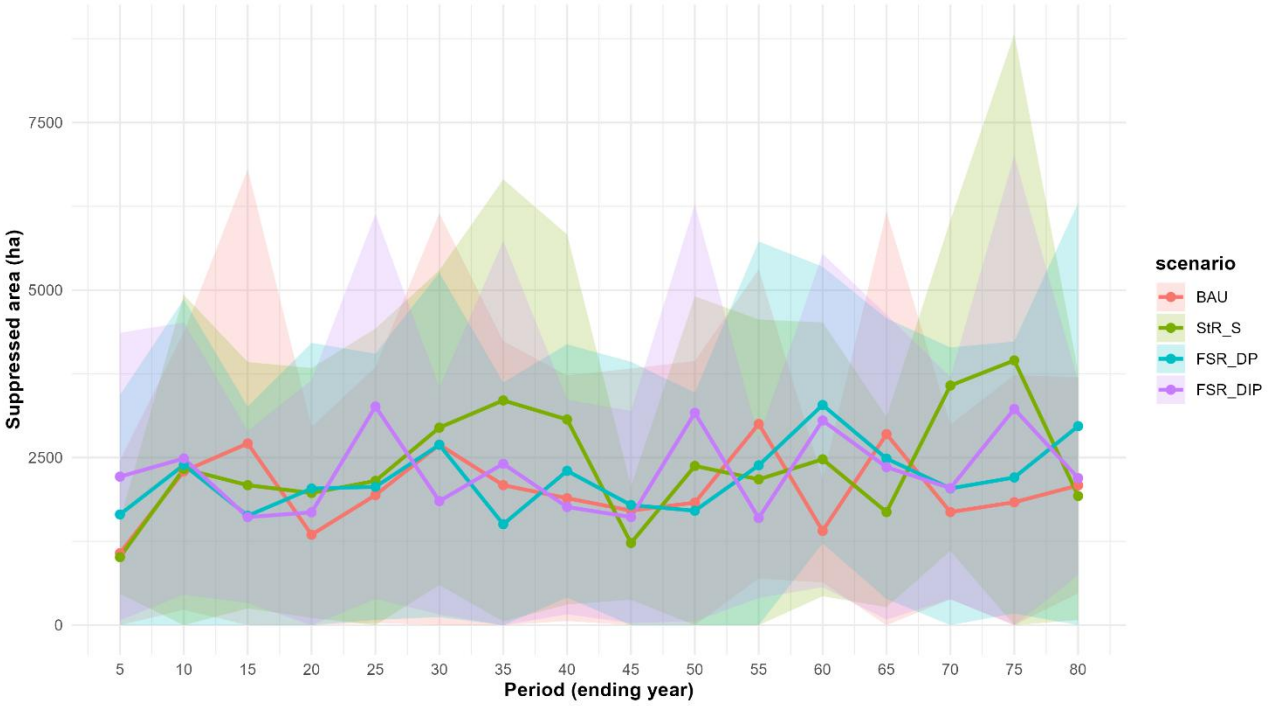

Figure 20. Total suppressed area (5-years totals; mean ± sd across runs: replicates for each scenario). Each point represents the sum of suppressed area in the previous 5 years. Results for the landscape: 1A1b

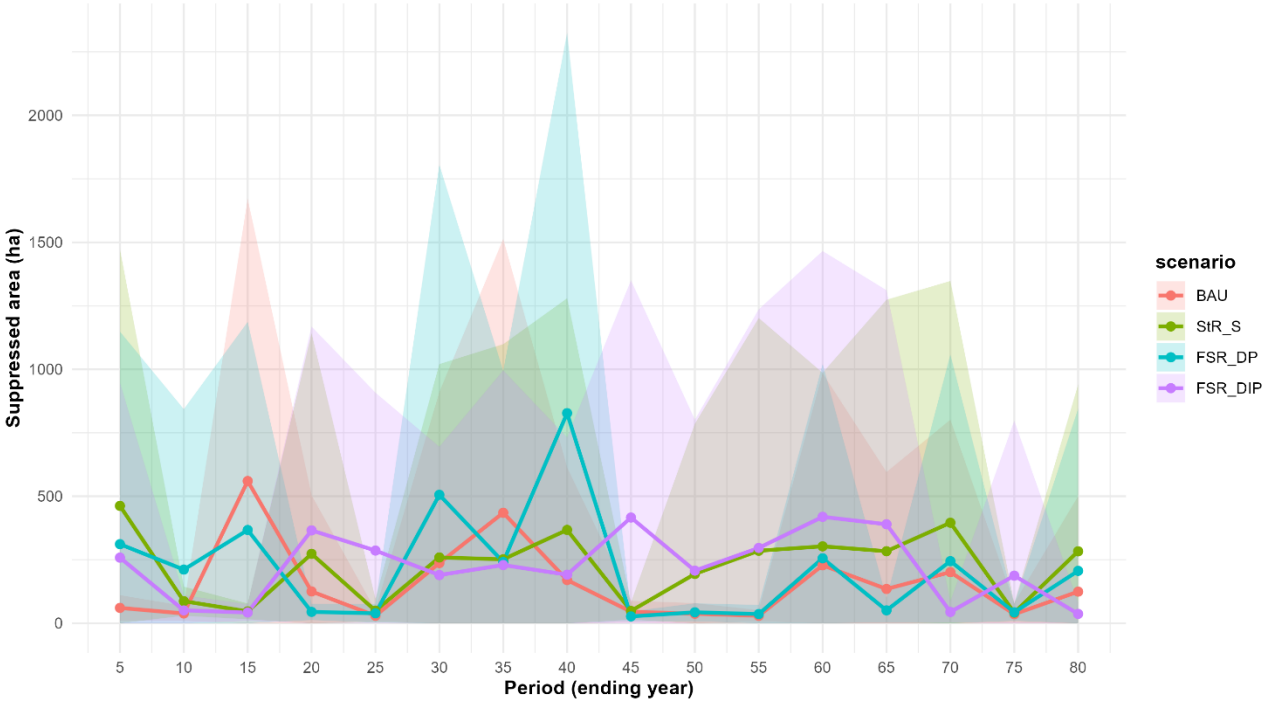

Figure 21. Total suppressed area (5-years totals; mean ± sd across runs: replicates for each scenario). Each point represents the sum of suppressed area in the previous 5 years. Results for the landscape: 1A2a

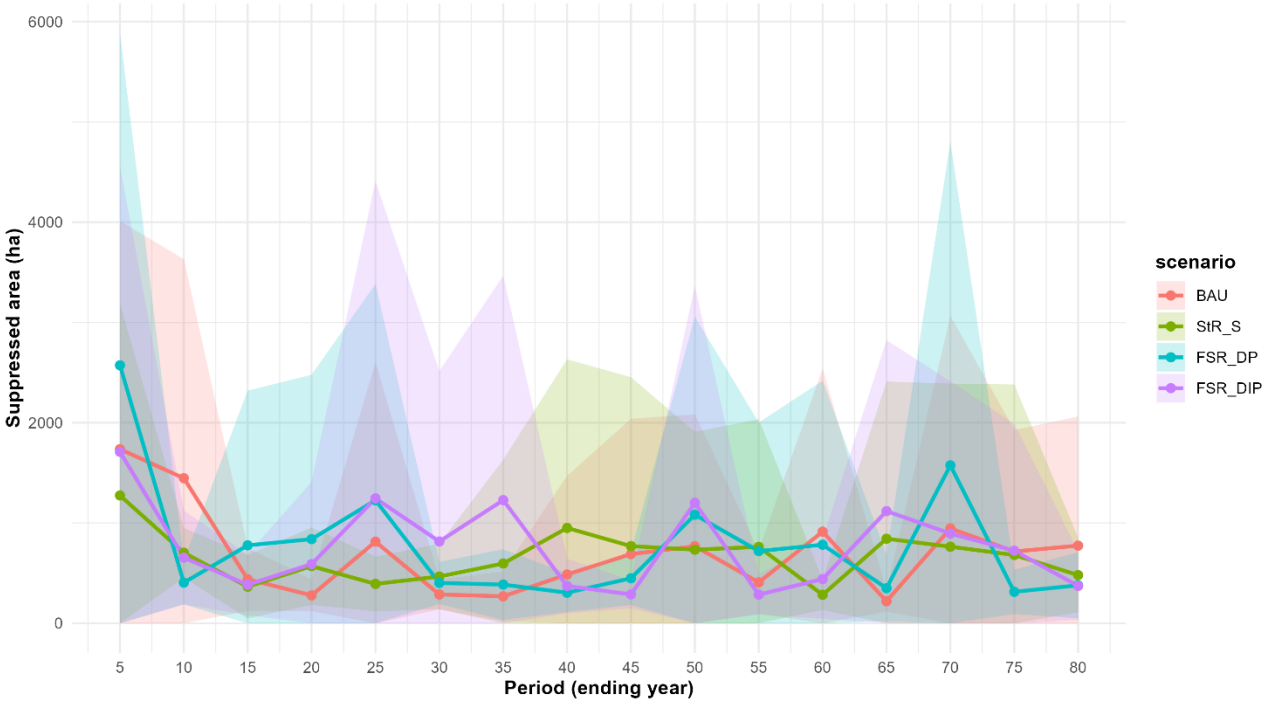

Figure 22. Total suppressed area (5-years totals; mean ± sd across runs: replicates for each scenario). Each point represents the sum of suppressed area in the previous 5 years. Results for the landscape: 1A2b

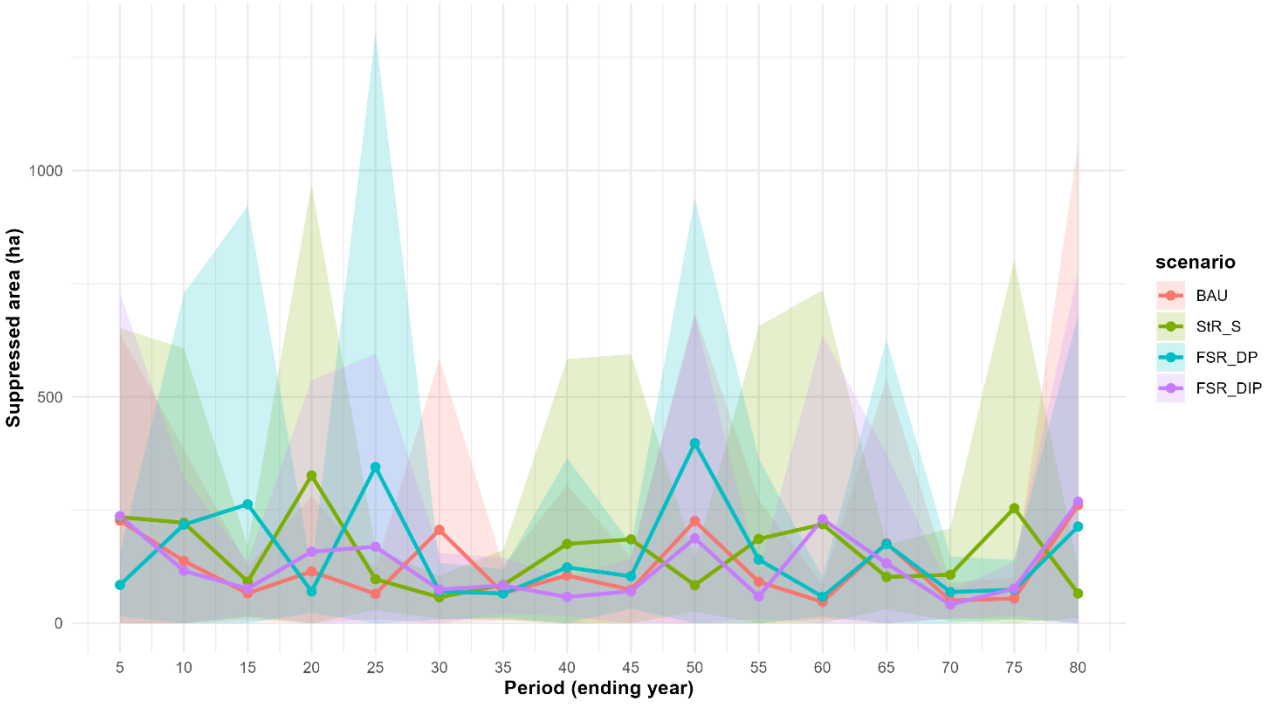

Figure 23. Total suppressed area (5-years totals; mean ± sd across runs: replicates for each scenario). Each point represents the sum of suppressed area in the previous 5 years. Results for the landscape: 1A2c

4.1.3. Total burned and suppressed area patterns comparison.

Suppressed area relative to burned area appears to follow a gradient across landscapes. In landscape 1A1b, suppressed area exceeds burned area in all scenarios throughout the simulation period (Figure 24). In landscape 1A2a, the difference is less pronounced (Figure 25), while in landscapes 1A2b and 1A2c, suppressed area generally remains lower than burned area (Figure 26 and 27).

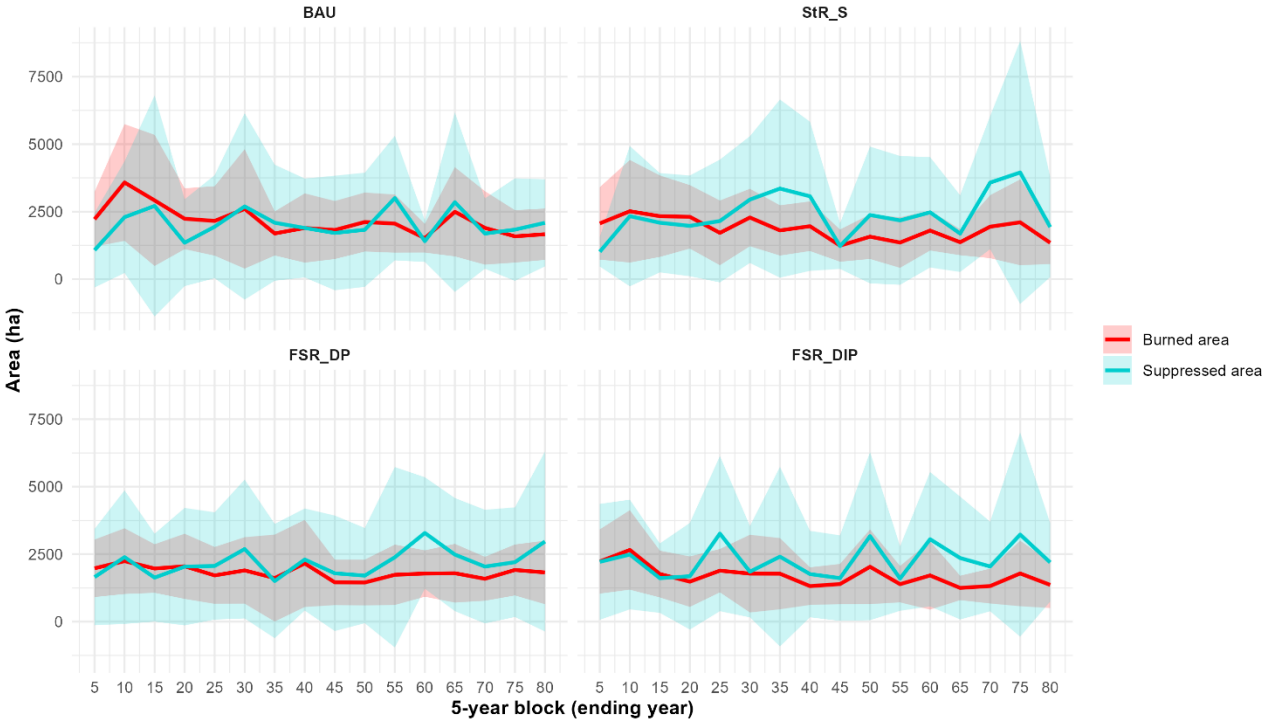

Figure 24. Burned vs suppressed area (5-years totals; mean ± sd across runs), across scenarios. Results for the landscape: 1A1b

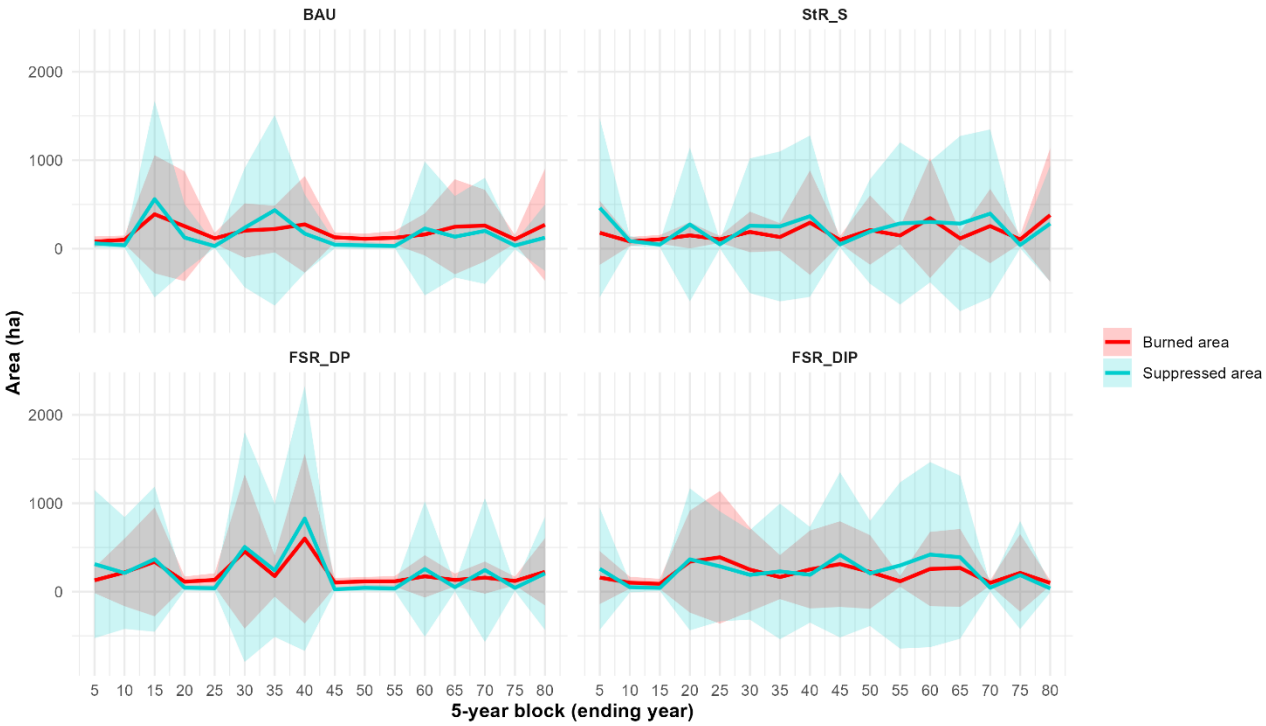

Figure 25. Burned vs suppressed area (5-years totals; mean ± sd across runs), across scenarios. Results for the landscape: 1A2a

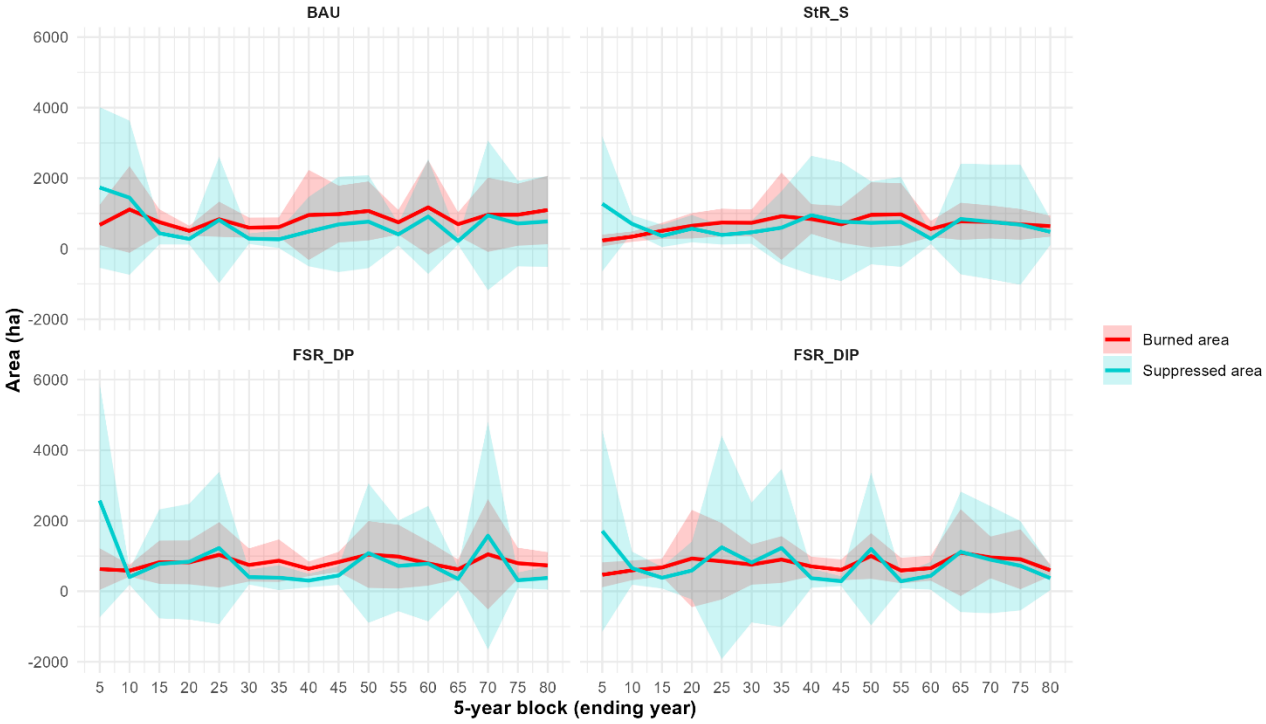

Figure 26. Burned vs suppressed area (5-years totals; mean ± sd across runs), across scenarios. Results for the landscape: 1A2b

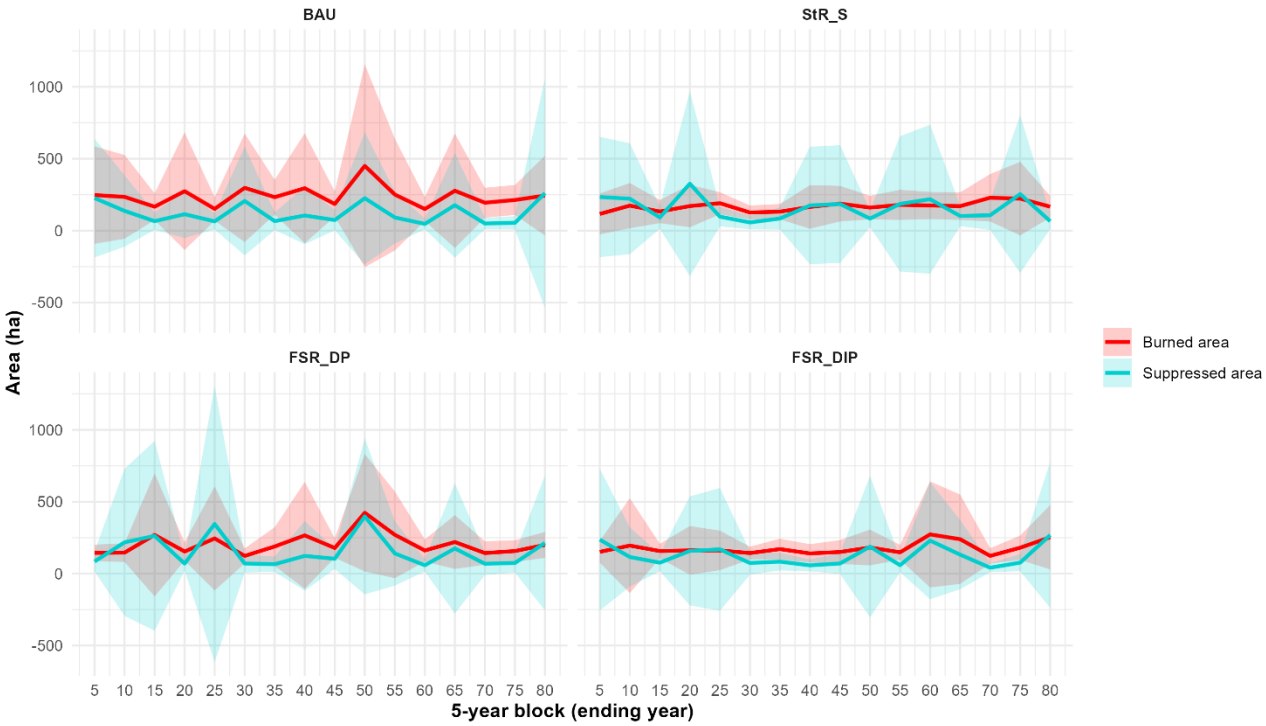

Figure 27. Burned vs suppressed area (5-years totals; mean ± sd across runs), across scenarios. Results for the landscape: 1A2c

4.1.4. Suppressed area types fraction.

The fraction of suppressed area types across scenarios is generally consistent across landscapes (Figure 28-31), and reflects the conditions defined for each scenario-. Firebreak suppression occurs only in FSR_DP and FSR_DIP scenarios, while mosaic suppression reaches higher values in FSR_DIP. Both firebreak and mosaic suppression are more frequent in 1A1b, likely because larger burned area increase the probability of intersecting firebreaks or crop areas (Figure 28).

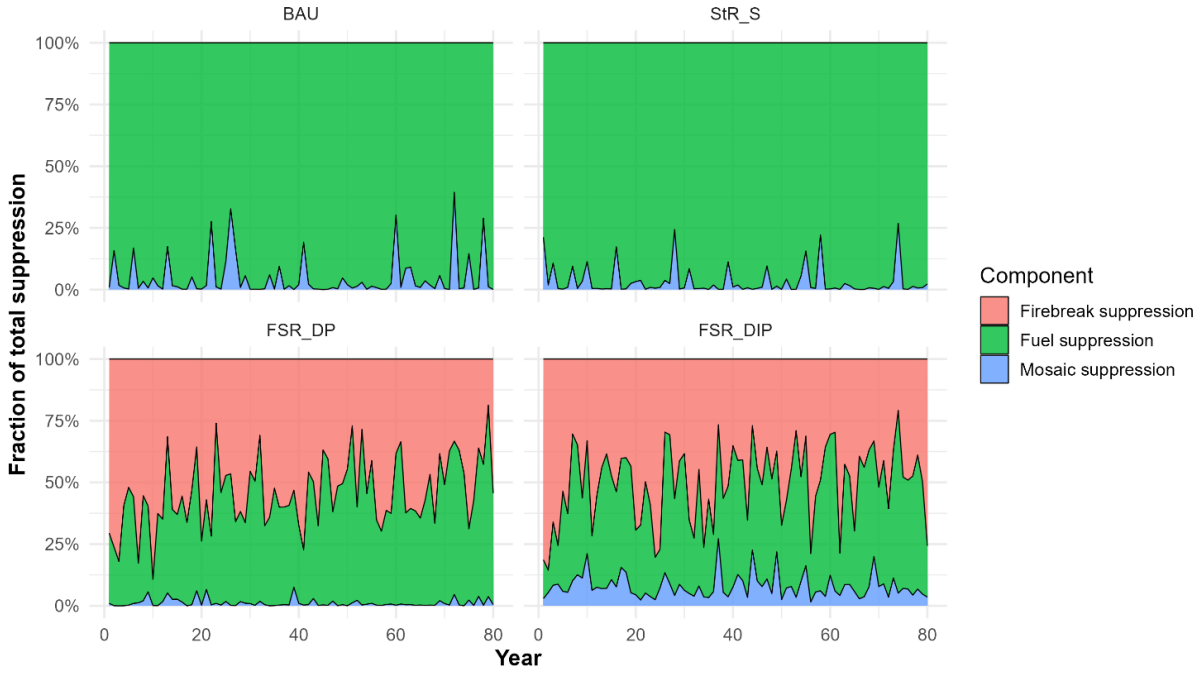

Figure 28. Fraction of suppression components per year, across scenarios. Results for 1A1b

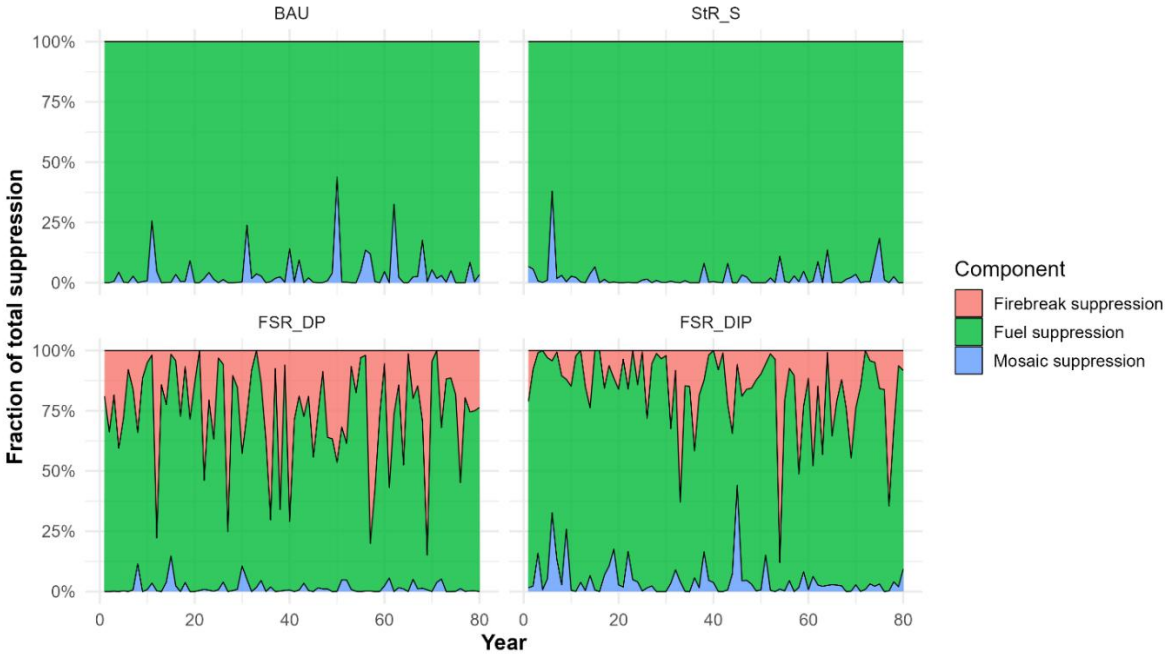

Figure 29. Fraction of suppression components per year, across scenarios. Results for 1A2a

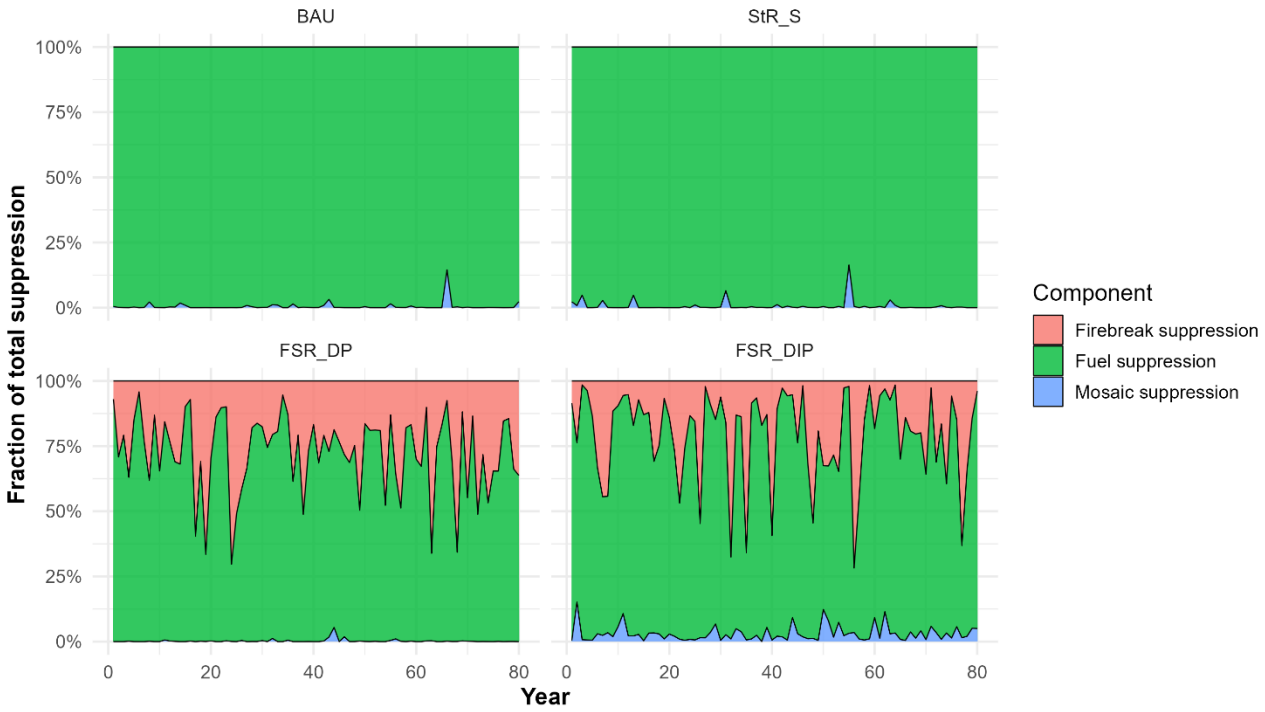

Figure 30. Fraction of suppression components per year, across scenarios. Results for the landscape: 1A2b

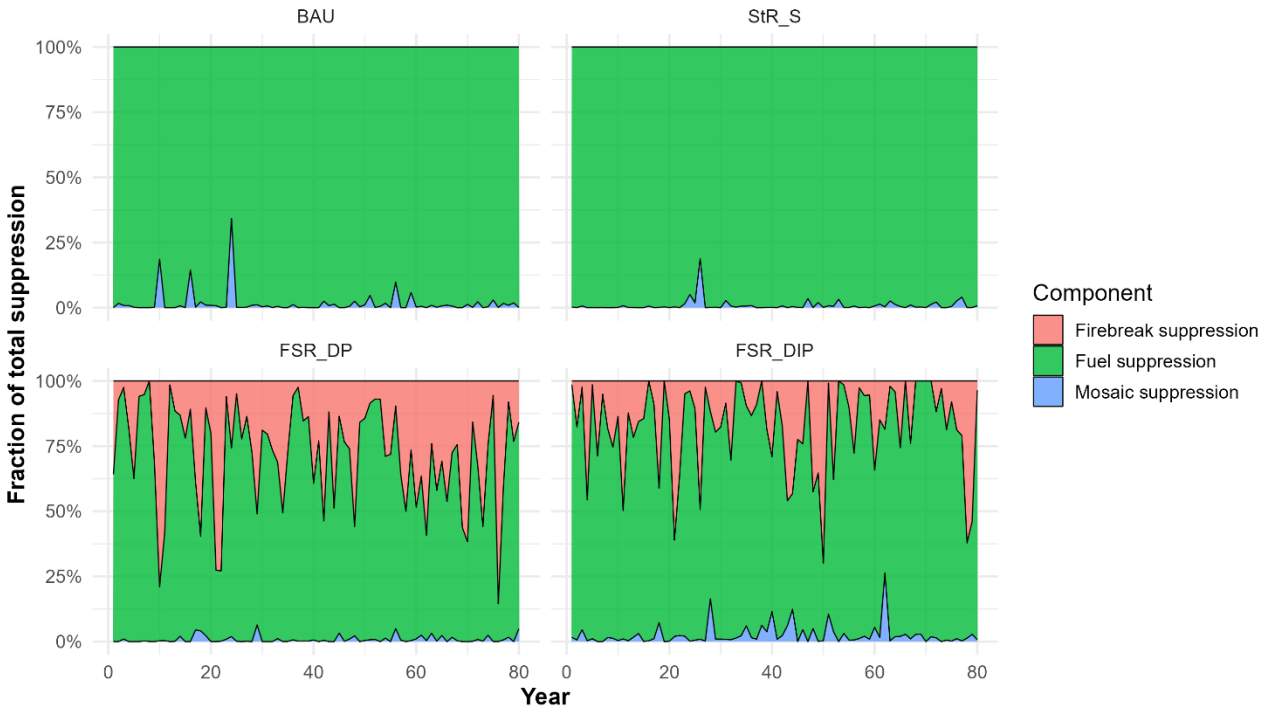

Figure 31. Fraction of suppression components per year, across scenarios. Results for 1A2c

4.1.5. Annual burned and suppressed area.

Annual values of burned and suppressed area show that across landscapes StR_S yields the highest values of fuel suppressed area, while the FSR scenarios are associated with highest firebreaks and mosaic suppression records (Figure 32-35).

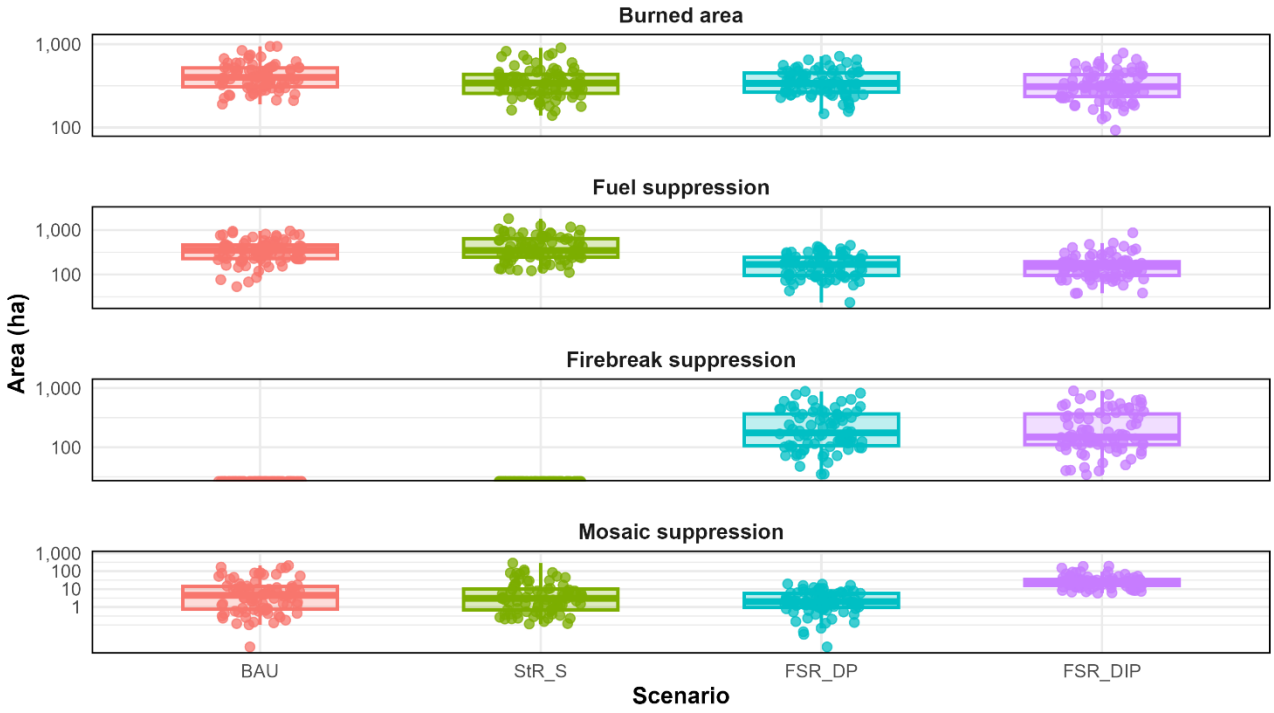

Figure 32. Annual burned and suppressed area (sum per year, averaged across runs), across scenarios. Results for the landscape: 1A1b

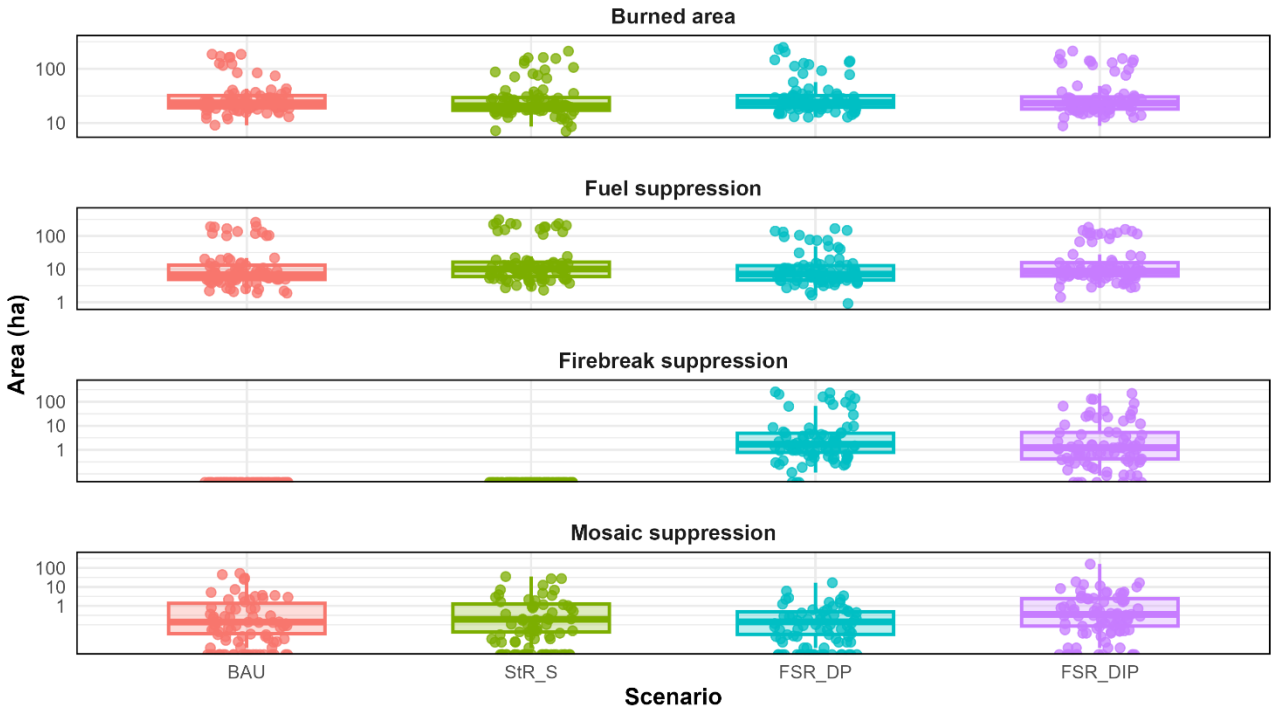

Figure 33. Annual burned and suppressed area (sum per year, averaged across runs), across scenarios. Results for the landscape: 1A2a

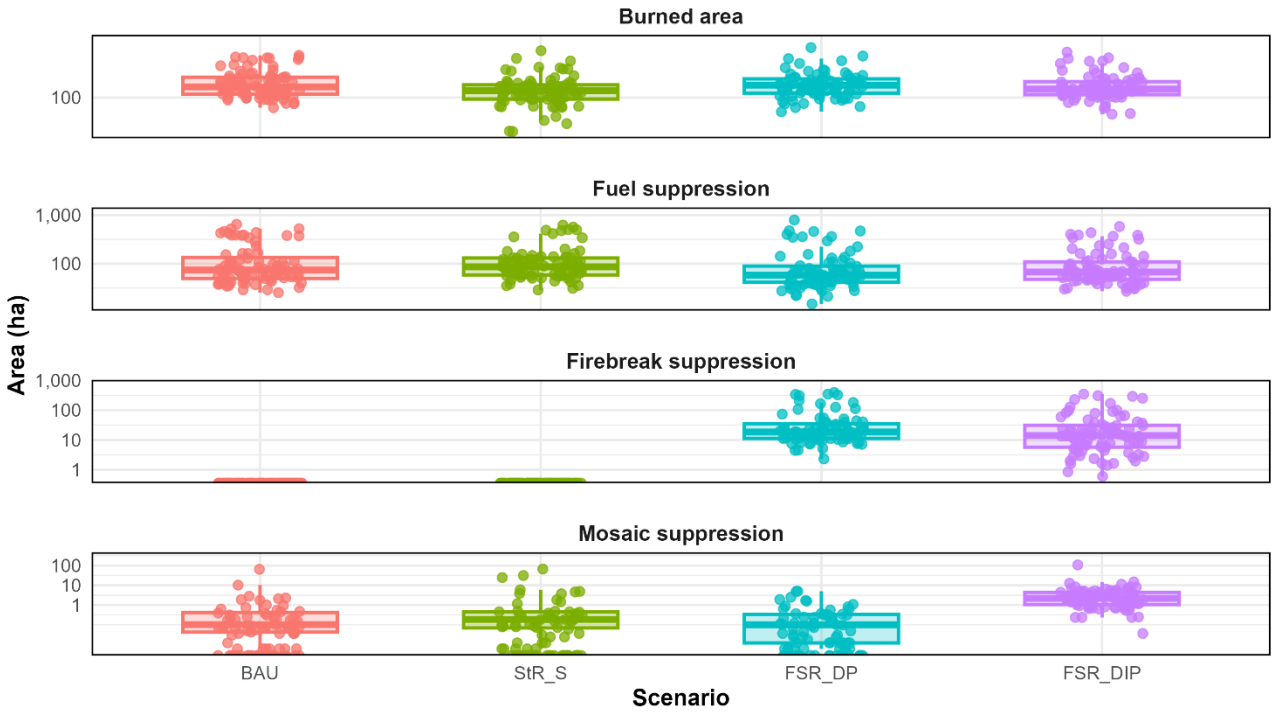

Figure 34. Annual burned and suppressed area (sum per year, averaged across runs), across scenarios. Results for the landscape: 1A2b

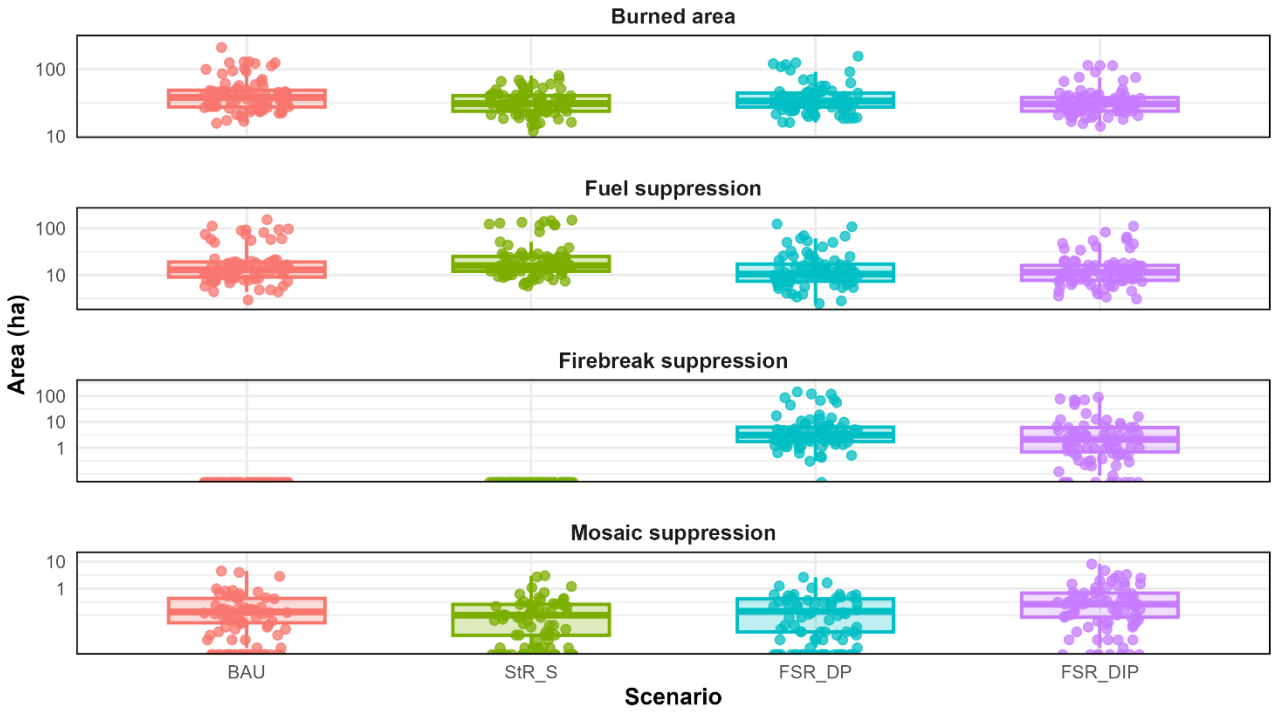

Figure 35. Annual burned and suppressed area (sum per year, averaged across runs), across scenarios. Results for the landscape: 1A2c

4.2. Forest age trends

4.2.1. Broadleaf and conifer age trends

FSR_DIP maintains consistently the lowest broadleaf age values across landscapes (Figure 36-39), although in landscape 1A1b, the BAU scenario shows lower values during the first years of the simulation (Figure 36). In landscape 1A2b and 1A2c, differences are less pronounced, but StR_S generally maintains the highest broadleaf ages (Figure 38 and 39), whereas in landscape 1A1b, the highest broadleaf ages are associated with FSR_DP (Figure 36). Similar patterns are observed for conifer age, which mirrors the trends seen for broadleaves (Figure 40-43). We interpret these results as a consequence of interacting processes parameterized in the model, including: higher fuel suppression in StR_S combined with no rejuvenating mechanisms, higher burned area in BAU, and mechanisms that rejuvenate or halt aging in FSR_DP and FSR_DIP (e.g. firebreaks, forest management and 5% to crop).

4.3 Summary tables

Mean results across simulation runs indicate that BAU scenario is consistently associated with the highest burned area, while FSR_DIP and FSR_DP record the lowest and second lowest burned areas, respectively (Table 10-13). StR_S consistently exhibits the highest suppressed area across all landscapes. Regarding fire size, mean fire size is largest in BAU or StR_S scenarios across all landscapes. Maximum fire size, however, varies by landscape: it occurs in BAU for landscapes 1A2b and 1A2c, in FSR_DP for 1A1b, and in FSR_DIP for 1A2a.

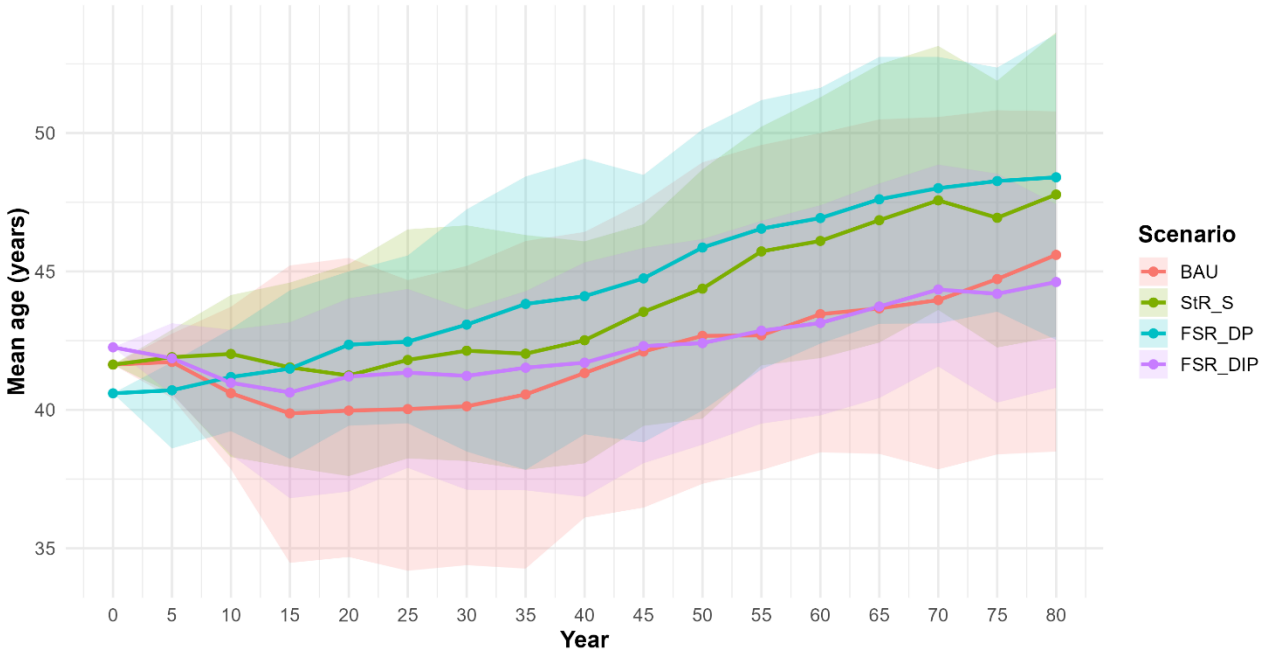

Figure 36. Broadleaf mean age (5-year mean; mean ± 10-90%). Results for the landscape: 1A1b

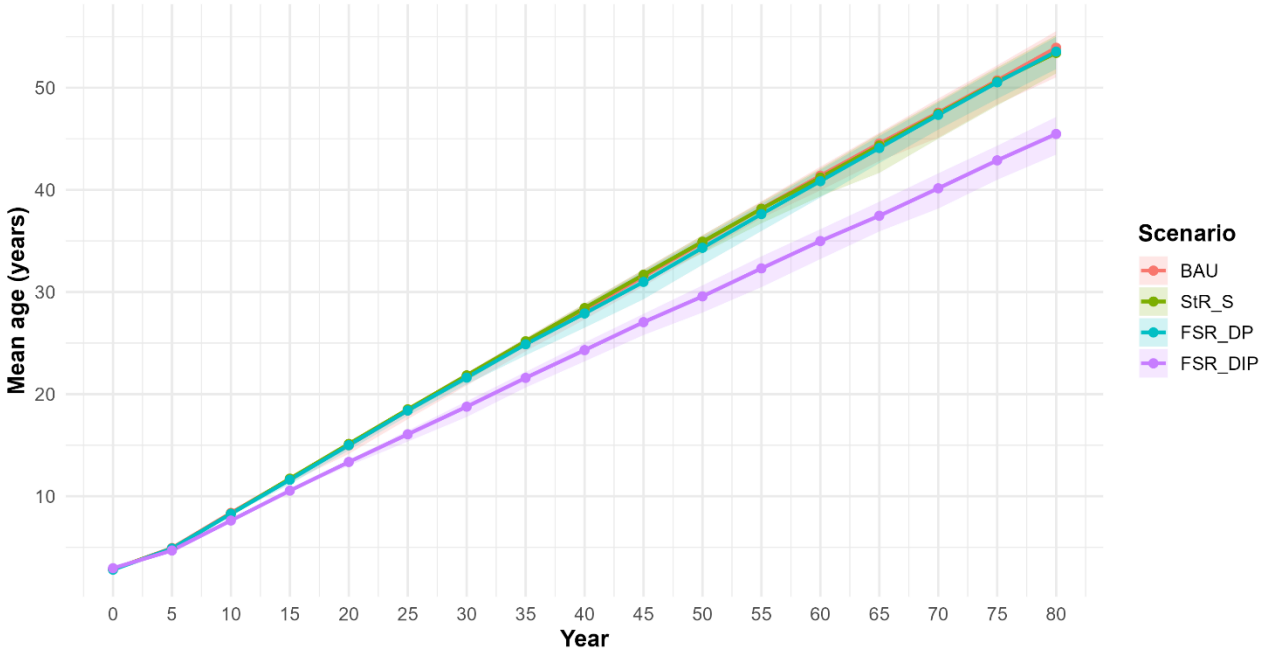

Figure 37. Broadleaf mean age (5-year mean; mean ± 10-90%). Results for the landscape: 1A2a

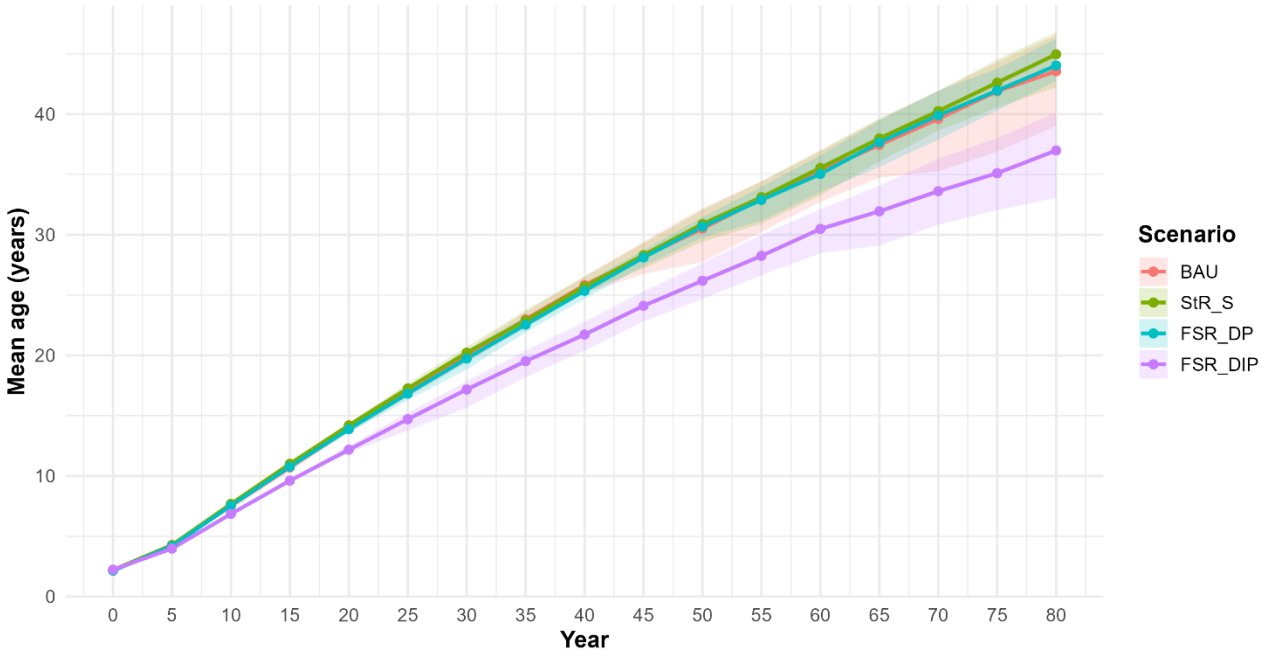

Figure 38. Broadleaf mean age (5-year mean; mean ± 10-90%). Results for the landscape: 1A2b

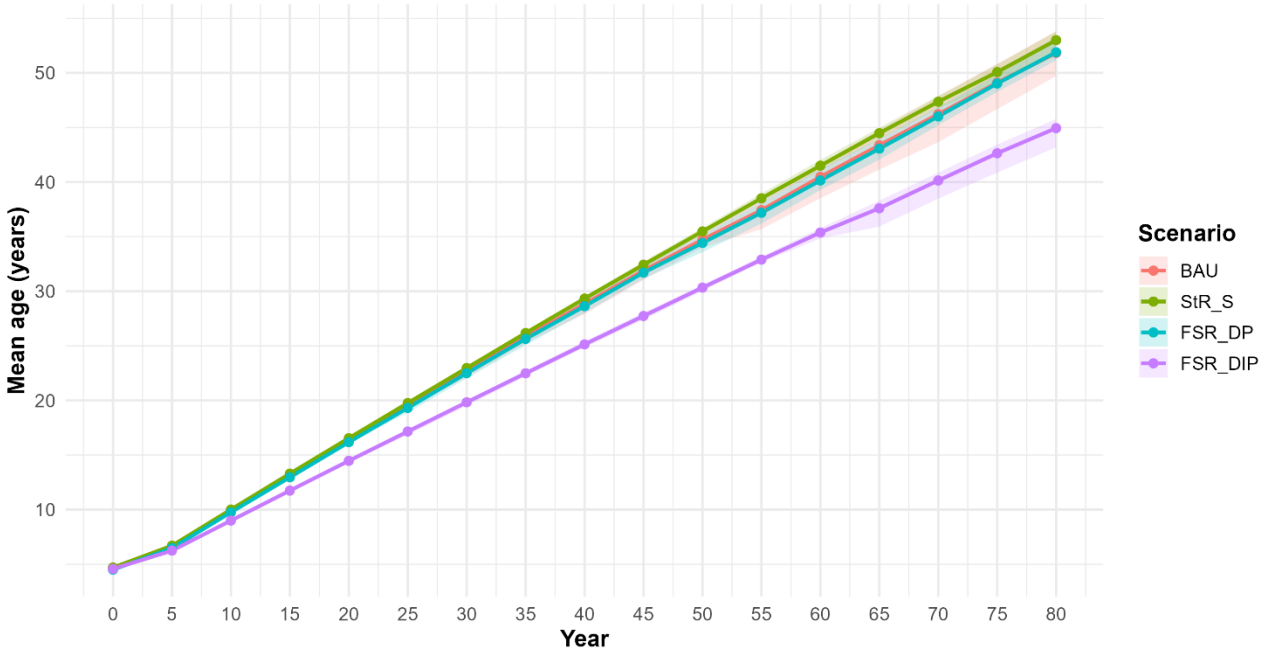

Figure 39. Broadleaf mean age (5-year mean; mean ± 10-90%). Results for the landscape: 1A2c

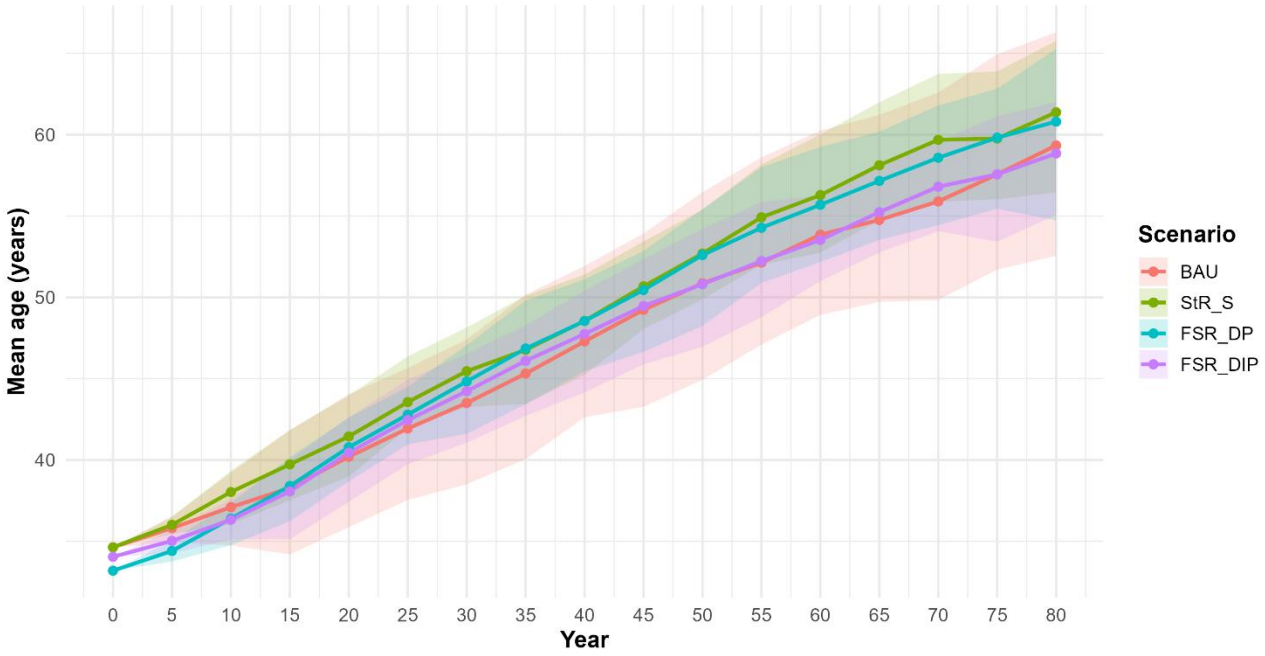

Figure 40. Conifer mean age (5-year mean; mean ± 10-90%). Results for the landscape: 1A1b

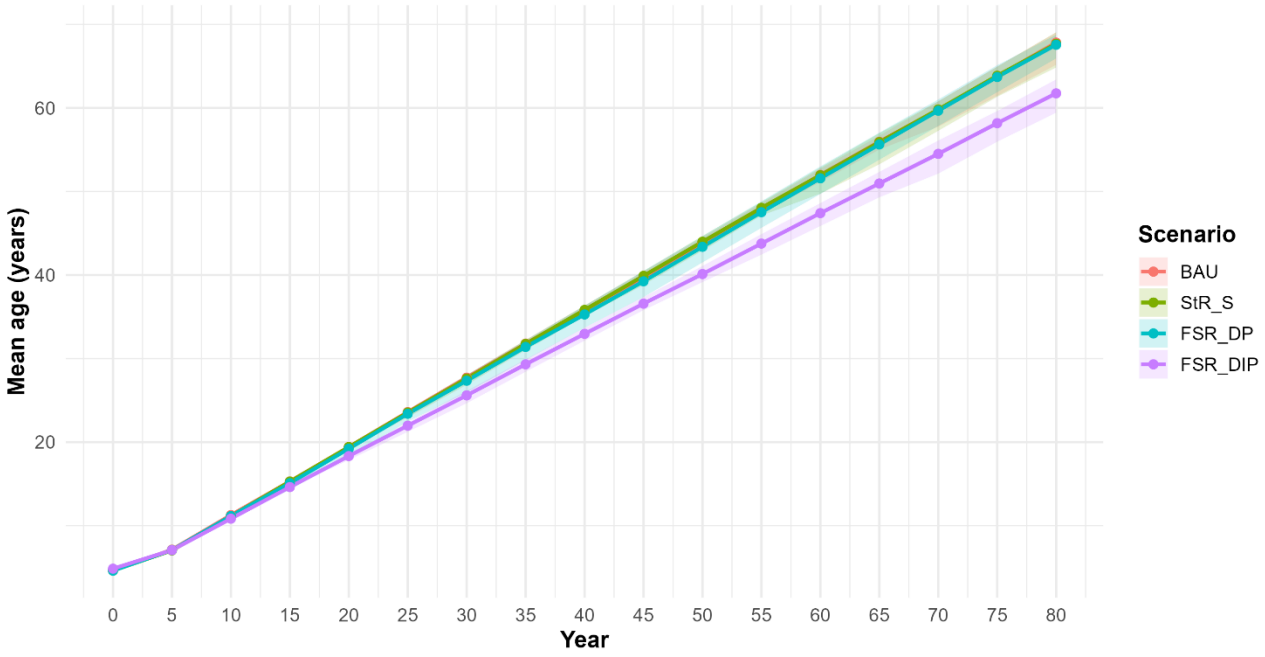

Figure 41. Conifer mean age (5-year mean; mean ± 10-90%). Results for the landscape: 1A2a

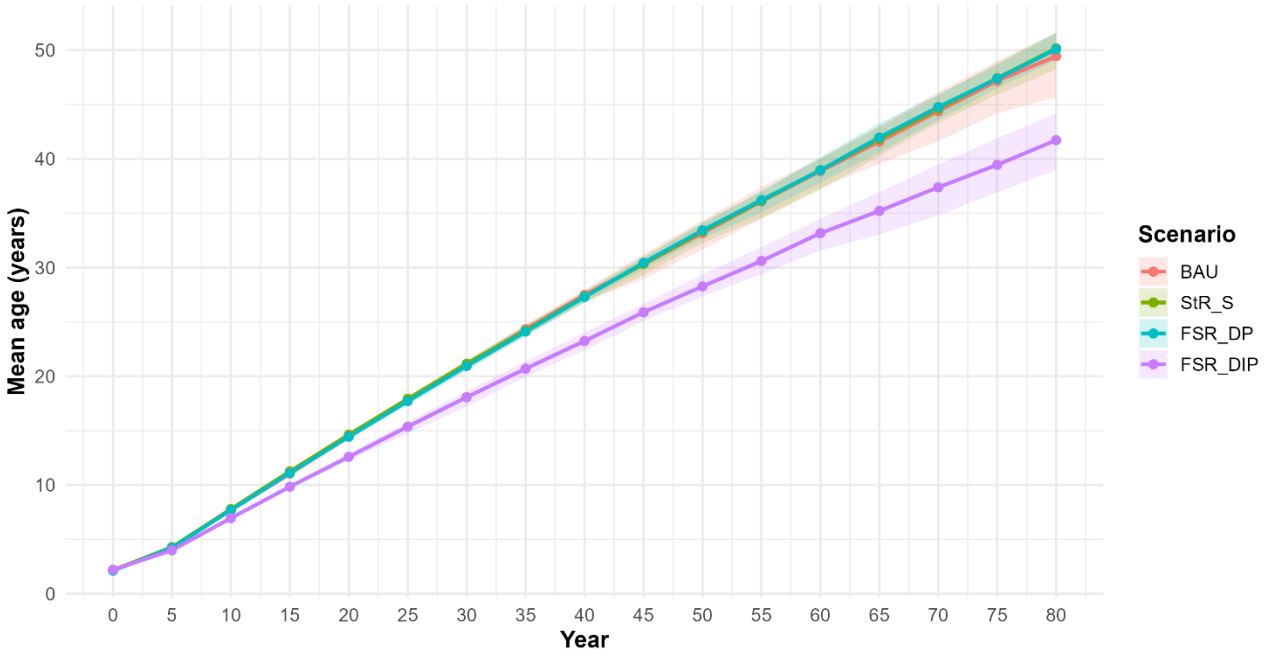

Figure 42. Conifer mean age (5-year mean; mean ± 10-90%). Results for the landscape: 1A2b

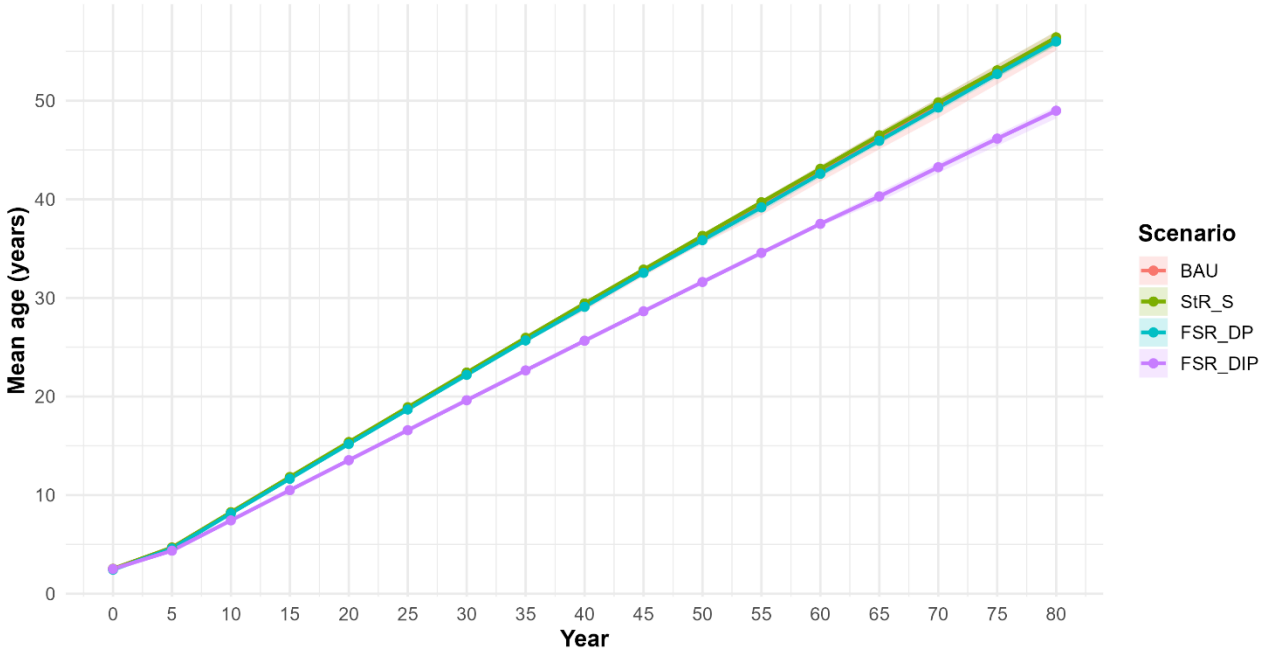

Figure 43. Conifer mean age (5-year mean; mean ± 10-90%). Results for the landscape: 1A2c

Table 10. Output variables (sum across years, mean across runs) across scenarios. BA = burned area; supp = suppressed; TOT/tot = total; REL = relative to sum of burned and suppresses area; sd = standard deviation; bla = broadleaf age; cona = conifer age; t0 = time step zero; tfinal = final time step; delta = difference between final and initial time step. Landscape: 1A1b

Variable	Unit	BAU	StR_S	FSR_DP	FSR_DIP
BA_TOT	ha	34444.49	29710.09	29178.70	27149.47
suppBA_fuel	ha	30820.74	37014.20	14538.32	14118.68
suppBA_mosaic	ha	1631.84	1308.14	305.03	2749.76
suppBA_firebreak	ha	0.00	0.00	20301.59	19673.00
suppBA_TOT	ha	32452.58	38322.34	35144.93	36541.45
suppBA_REL	%	0.49	0.56	0.55	0.57
fire_size_max	ha	1154.25	751.05	1326.96	1071.45
fire_size_mean	ha	11.48	9.66	10.05	9.25
fire_size_median	ha	6.03	5.67	5.85	5.58
fire_size_sd	ha	28.90	20.14	21.87	18.57
tot_bla_t0	ha*years	1221921.00	1221921.00	1191466.26	1180851.48
tot_bla_tfinal	ha*years	1438097.11	1505185.62	1516277.34	1351871.37
tot_bla_delta	ha*years	216176.11	283264.62	324811.08	171019.89
tot_cona_t0	ha*years	137069.82	137069.82	131379.66	130473.00
tot_cona_tfinal	ha*years	205430.83	221511.04	227010.97	210653.75
tot_cona_delta	ha*years	68361.01	84441.22	95631.31	80180.75

Table 11. Output variables (sum across years, mean across runs) across scenarios. BA = burned area; supp = suppressed; TOT/tot = total; REL = relative to sum of burned and suppresses area; sd = standard deviation; bla = broadleaf age; cona = conifer age; t0 = time step zero; tfinal = final time step; delta = difference between final and initial time step. Landscape: 1A2a

Variable	Unit	BAU	StR_S	FSR_DP	FSR_DIP
BA_TOT	ha	97114.32	97114.32	95777.82	95578.56
suppBA_fuel	ha	1893360.88	1879714.72	1889420.83	1536483.23
suppBA_mosaic	ha	1796246.56	1782600.40	1793643.01	1440904.67
suppBA_firebreak	ha	0.00	0.00	3854.16	3849.30
suppBA_TOT	ha	56833.36	56957.66	56411.89	48947.82
suppBA_REL	%	52965.70	53090.00	52557.73	45098.52
fire_size_max	ha	3052.13	2897.62	3308.80	3331.92
fire_size_mean	ha	2298.22	3487.22	1651.22	2314.60
fire_size_median	ha	194.41	145.30	46.53	300.94
fire_size_sd	ha	0.00	0.00	1757.37	995.07
tot_bla_t0	ha*years	2492.62	3632.51	3455.12	3610.61
tot_bla_tfinal	ha*years	0.45	0.56	0.51	0.52
tot_bla_delta	ha*years	881.37	1381.77	503.28	693.81
tot_cona_t0	ha*years	7.77	7.28	7.60	6.86
tot_cona_tfinal	ha*years	4.77	4.14	4.41	4.14
tot_cona_delta	ha*years	18.01	26.05	17.20	15.57

Table 12. Output variables (sum across years, mean across runs) across scenarios. BA = burned area; supp = suppressed; TOT/tot = total; REL = relative to sum of burned and suppresses area; sd = standard deviation; bla = broadleaf age; cona = conifer age; t0 = time step zero; tfinal = final time step; delta = difference between final and initial time step. Landscape: 1A2b

Variable	Unit	BAU	StR_S	FSR_DP	FSR_DIP
BA_TOT	ha	66308.22	66308.22	64580.40	63707.76
suppBA_fuel	ha	1366557.43	1414124.21	1392462.76	1113162.28
suppBA_mosaic	ha	1300249.21	1347815.99	1327882.36	1049454.52
suppBA_firebreak	ha	0.00	0.00	13300.02	13147.20
suppBA_TOT	ha	281675.76	295076.36	288001.44	226886.34
suppBA_REL	%	268093.68	281494.28	274701.42	213739.14
fire_size_max	ha	13751.26	11035.34	12986.65	12294.47
fire_size_mean	ha	11095.12	10476.25	8521.98	8743.11
fire_size_median	ha	95.08	156.74	26.83	351.83
fire_size_sd	ha	0.00	0.00	4015.17	3228.10
tot_bla_t0	ha*years	11190.19	10632.99	12563.98	12323.03
tot_bla_tfinal	ha*years	0.45	0.49	0.49	0.50
tot_bla_delta	ha*years	1061.01	618.30	763.74	1155.51
tot_cona_t0	ha*years	10.00	8.27	9.13	9.09
tot_cona_tfinal	ha*years	5.58	4.59	5.31	4.77
tot_cona_delta	ha*years	24.46	15.52	19.04	22.57

Table 13. Output variables (sum across years, mean across runs) across scenarios. BA = burned area; supp = suppressed; TOT/tot = total; REL = relative to sum of burned and suppresses area; sd = standard deviation; bla = broadleaf age; cona = conifer age; t0 = time step zero; tfinal = final time step; delta = difference between final and initial time step. Landscape: 1A2c

Variable	Unit	BAU	StR_S	FSR_DP	FSR_DIP
BA_TOT	ha	73897.02	73897.02	70858.98	68394.96
suppBA_fuel	ha	885039.35	895706.50	882012.31	732454.04
suppBA_mosaic	ha	811142.33	821809.48	811153.33	664059.08
suppBA_firebreak	ha	0.00	0.00	38860.02	37982.52
suppBA_TOT	ha	925363.39	941346.54	927863.58	771579.10
suppBA_REL	%	885066.43	901049.58	889003.56	733596.58
fire_size_max	ha	3867.29	2700.38	3290.58	2832.02
fire_size_mean	ha	1945.71	2477.08	1459.97	1366.72
fire_size_median	ha	23.11	15.81	16.50	50.91
fire_size_sd	ha	0.00	0.00	996.23	620.09
tot_bla_t0	ha*years	1968.82	2492.89	2472.70	2037.72
tot_bla_tfinal	ha*years	0.34	0.48	0.43	0.42
tot_bla_delta	ha*years	624.69	176.40	672.93	363.78
tot_cona_t0	ha*years	8.04	6.46	7.40	6.78
tot_cona_tfinal	ha*years	5.40	4.23	4.77	4.41
tot_cona_delta	ha*years	13.96	8.98	15.54	10.17

4.4 Multivariate analysis

Principal component analysis applied to results from all runs and landscapes at the beginning (time step = +5 years) and at the end of the simulation (time step = +80 years) shows that the first axis is strongly related to forest age at both time steps, but in opposite directions: it is inversely related at the beginning (Figure 44) and directly related at the end of the simulation (Figure 45). Similarly, the second axis reflects a gradient related to fire dynamics: it is positively associated with the relative burned area over the total potential burned area, and inversely associated with the suppressed burned area relative to the total potential burned area (note that these two variables are inversely correlated by definition).

Interestingly, at the beginning of the simulation, total burned area and mean forest age are correlated, as both load on the same side of the first axis, whereas after 80 years they load in opposite directions. A similar pattern is observed for median and maximum fire size, which are aligned with forest age at the beginning of the simulation but show an opposite relationship at the end (Figure 45). This pattern may reflect the mechanism by which fire rejuvenates forests by reducing stand age by one age class. Consequently, higher burned areas force many landscape cells to lose age classes, leading to a reduction in mean forest age at the landscape scale.

Regarding the position of the landscapes in the biplot space, they are located as expected at the beginning of the simulation. Landscape 1A1b is characterised by older forest ages but also by a larger absolute burned area, whereas landscapes 1A2a, 1A2b, and 1A2c are positioned at the opposite end of the first axis, representing landscapes with younger forest ages due to more recent abandonment (see Deliverable 1.1).

After 80 years of simulation, landscape 1A1b shows a lower mean age, as it has experienced a larger burned area, while landscapes in which fire played a more limited role have aged more substantially. These results highlight the potential of landscape-scale fires to reduce forest ageing processes, bringing forests back to or maintaining them in younger developmental stages, with implications also for landscape-scale carbon stock potential (see Deliverable 3.2).

Regarding the scenarios, after 80 years of simulation both the SrT_S and FSR_DP scenarios show a correlation with an increase in mean landscape age, that is, the realization of forest ageing (i.e., a proforestation policy). This likely depends on the strong leverage that the fuel suppression mechanism has on the final burned area. In fact, the suppressed burned area is highly sensitive to this mechanism within REMAINS, and consequently an increase in fuel suppression potential leads to a lower relative burned area and thus to greater forest ageing.

Moreover, in SrT_S there are no rejuvenation mechanisms linked to higher levels of management (i.e., firebreaks, higher management quotas of forests and pastures, and increased crop proportion). In contrast, in FSR_DP a rejuvenation effect is present due to firebreaks, where forest age is reduced by one class and cells do not age over 2% of the total landscape area. However, despite the reduced investment in fuel suppression in this scenario, firebreaks are able to compensate by further contributing to the reduction of the final burned area through the firebreak suppression mechanism. Nevertheless, unlike the FSR_DIP scenario—where an additional rejuvenation occurs over a further 5% of the landscape converted to crops to meet the mosaic suppression strategy—in FSR_DP no additional rejuvenation takes place. As a result, forests are still able to age following a trajectory similar to that observed in SrT_S.

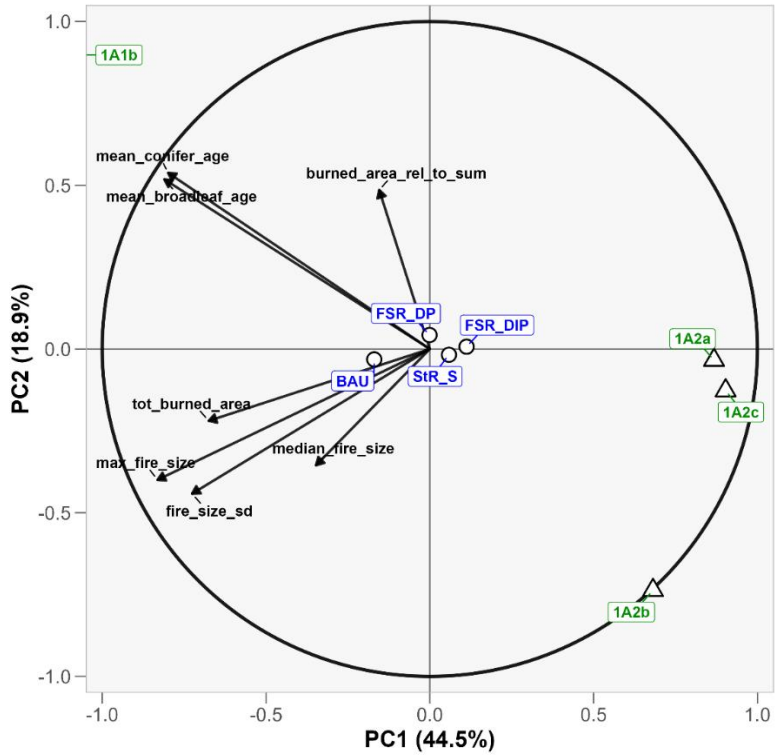

Figure 44. PCA over all simulated runs for years 1-20 (first 20 years of the simulation). Landscapes are shown in green, while scenarios are shown in blue.

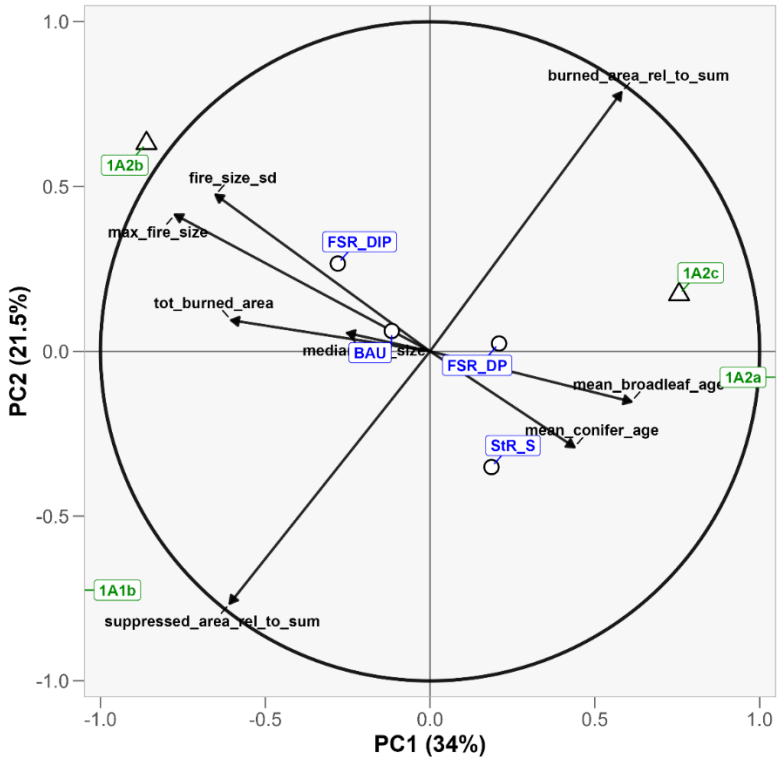

Figure 45. PCA over all simulated runs for years 61-80 (last 20 years of the simulation). Landscapes are shown in green, while scenarios are shown in blue.

5. Discussions

The rationale of REWILD-FIRE starts from a tension that has become central to European rewilding policies: natural reforestation of abandoned agro-pastoral land and proforestation can rapidly increase carbon stocks, yet the same biomass accumulation dynamics (particularly the dead component) can amplify the probability of large wildfires and thus erode, in the mid- to long term, a substantial share of the "carbon gain" through fire-induced emissions and the loss of stocks. This critical issue is especially relevant in the Alpine context, where the increase in forest cover and the reduction of management rates over recent decades combine with signals of increasing fire frequency and severity under climate extremes (Valese et al. 2014). In this framework, the REWILD-FIRE project represents a methodological attempt to test with a simulation experiment policy scenario calibrated on real data. In particular, Deliverable 3.1 it builds and parameterises a modelling chain able to link (i) climatic drivers and historical fire information, (ii) fuel structure and continuity shaped by stand age, management, and rewilding, and (iii) suppression and prevention strategies (direct and indirect), producing indicators that are comparable across scenarios and Alpine landscapes.

Deliverable 3.1 formalises the idea that there is no "rewilding" that is neutral with respect to disturbance regimes: forest ageing and the spontaneous transition from croplands/pastures to woody vegetation increase stocks and sink potential, but also act on fire susceptibility and hence the likelihood of severe events in the future. The innovative element is that these processes are not treated as separate components, but as parts of the same dynamic system in which stand age is a proxy for both carbon and fuel load accumulation and connectivity at the landscape scale. In REMAINS, "time since change" becomes a major driver of changes. Any choice that increases mean stand age (e.g., proforestation or abandonment of management) tends to increase stocks and, simultaneously, to modify fire susceptibility, spread and growth. Conversely, fire can rejuvenate portions of the landscape by lowering age classes or imposing post-fire transitions.

This architecture responds directly to the concerns raised in the project proposal: avoiding short-sighted policies that maximise sinks without considering disturbance dynamics and that, under climate extremes, may favour conflagrations capable of partially offsetting additional sequestration. The deliverable therefore provides an operational platform to move from a binary "rewilding yes/no" debate to "fire-smart rewilding", i.e., rewilding compatible with wildfire-risk mitigation goals.

5.1 Climate drivers, uncertainty, and burned area distributions

A major methodological component of Deliverable 3.1 concerns the generation of future burned area (BA) distributions from Fire Weather Index (FWI) and the empirical relationship between meteorological indices and observed BA. This analysis highlights both the value and the limitations of using FWI as a driver of BA at landscape scale. The weak relationship observed between aggregated seasonal or annual FWI values and BA is consistent with the fact that FWI captures only the meteorological dimension of fire danger. In contrast, BA results from the interaction among multiple factors: ignition pressure, fuel amount and continuity, land management, suppression efficiency, and short-lived episodes of extreme conditions that may or may not coincide with ignitions. In practice, years with high fire danger may still exhibit limited BA if ignitions are rare or quickly contained. Conversely, years with moderate fire-weather conditions can generate large BA when ignition timing coincides with dry fuels and adverse wind patterns, or when suppression capacity is exceeded. These findings suggest that climate-driven indices are generally more effective

at describing the *potential for fire spread* than the realized burned area, particularly when analysed at annual resolution and in regions where human factors strongly influence fire outcomes.

A second issue concerns temporal and spatial aggregation. Annual or seasonal averages of FWI tend to dilute the signal conveyed by high-end tail events, although such events may be disproportionately responsible for large BA. To partially address this limitation, our workflow aligned predictors with the relevant fire season (October to March) and incorporated metrics designed to capture both "background" danger (seasonal means) and extremes (seasonal peaks and high quantiles such as fwi_max_p99-like indicators). Nevertheless, monthly aggregation inevitably smooths the short-lived daily peaks that often control fire growth (for example, wind-driven spread occurring over just a few days). This helps explain why the empirical model is able to reproduce central tendencies but struggles to capture the observed multi-modality and full dispersion of the observed BA distributions. Moreover, the observation period is relatively short (2007–2024), resulting in a limited effective calibration sample. This constrains the model's ability to robustly infer the relationship between rare extreme conditions and realised BA, particularly in the upper tail of the distribution.

Model structure is another key determinant of our results. We adopted ridge regression on log1p(BA), including landscape fixed effects, in order to stabilise inference in the presence of multicollinearity among predictors and persistent between-landscape differences (e.g., fuels, access, suppression capacity). Regularisation reduces overfitting and enhances the stability of projections; however, it also shrinks coefficients towards zero, potentially dampening model sensitivity to extreme conditions. At the same time, the back-transformation from log scale may inflate the right tail of the distribution when predictors move beyond their historical range. This effect is visible in some scenario–GCM combinations, where simulated BA distributions exhibit heavier upper tails than those observed. Such behaviour does not necessarily imply a genuine physical increase in variability. Rather, it may arise from extrapolation of an empirical model and from structural differences between reanalysis-based FWI and bias-corrected projected FWI, even when mean and variance are aligned over a reference period. For this reason, it is essential to verify whether future predictor values fall outside the calibration envelope. When this occurs, extrapolation should be explicitly constrained (for example by capping predictors to historical maxima, adopting spline or threshold models, or fitting a model explicitly designed for extremes).

Inter-model spread emerges as another dominant source of variability. Differences between HadGEM2-ES and CNRM-CM5 in both mean and tail behaviour of FWI translate directly into divergent BA distributions, often exceeding the difference between RCP4.5 and RCP8.5 over the mid-century horizon. This highlights that uncertainty in regional fire-weather projections can be as influencial as scenario choice, and that results should be communicated as an ensemble of plausible futures rather than a single deterministic trajectory. The distributional approach used here (fitting parametric forms to the simulated annual BA in 2025–2064) is useful for this purpose: it provides a compact, transferable description of expected BA variability that can be sampled in downstream risk assessments, and it makes clear whether projected changes are driven by shifts in central tendency, changes in spread, or changes in tail heaviness.

A key discrepancy persists between observed and simulated BA distributions. Observations are typically flatter and more multi-modal, reflecting the influence of heterogeneous drivers and regime shifts within the observation period (for instance, changes in ignition patterns, land use, or suppression policy, and clustered fire years driven by a few major events). By contrast, the simulated BA distributions are derived from a climate-only predictor set with a stationary statistical mapping,

which tends to yield smoother, unimodal shapes. This is an expected limitation of purely meteorology-based models and reinforces that these projections represent *climate-conditioned potential BA* under stationary non-climatic controls, not a full forecast of realized BA.

Overall, the analysis provides a transparent, reproducible framework for translating fire-weather projections into BA distributions, while explicitly quantifying uncertainty across scenarios and climate models. Its main strengths include: (i) seasonally consistent aggregation, (ii) inclusion of extreme-sensitive predictors, (iii) regularised calibration to reduce instability, and (iv) distributional reporting that supports Monte Carlo sampling. At the same time, several caveats must be aknowledged: (i) limited calibration length and rare-event information, (ii) partial smoothing of daily extremes due to monthly inputs, (iii) non-stationarity in ignition and suppression not represented in the model, and (iv) potential extrapolation artefacts when projected FWI exceeds the historical range.

5.2 Burned area, forest age, fire-driven regeneration, and implications for the project hypothesis

The four simulated scenarios (BAU; Strict Rewilding + Suppression, StR_S; Fire-Smart Rewilding + Direct Prevention, FSR_DP; Fire-Smart Rewilding + Direct + Indirect Prevention, FSR_DIP) are explicitly designed to represent the policy alternatives targeted by REWILD-FIRE project: largely unplanned rewilding, a response primarily centred on suppression, and strategies that combine rewilding with active prevention and landscape management (e.g., firebreaks and agromosaic).

The results display an overall pattern consistent with the project's core hypothesis: BAU scenario generally yields the highest total BA, whereas FSR_DIP and FSR_DP show lower BA levels, with FSR_DIP typically performing best and FSR_DP second. In the most flammable landscape (1A1b), the combination of direct and indirect prevention measures appears capable of reducing BA consistently throughout the entire simulation period, suggesting that landscape-level fuel management can substantially mitigate fire outcomes even under challenging fire-weather conditions.

The StR_S scenario—combining "strict" rewilding with increased suppression— was expected to reveal a negative feedback known as the "fire-fighting trap" (Moreira et al. 2020). In this mechanism, higher suppression capacity increases the area effectively "suppressed" and can reduce relative BA, but it also risks promoting fuel accumulation (as vegetation continues to age and fire is partially or selectively excluded), thereby creating conditions for larger fires when suppression fails or is overwhelmed. However, the simulation did not reproduce this mechanism. While the SrT_S exhibited the highest suppression rates compared to the other scenarios, it did not show the typical temporal patterns associated with the "fire-fighting trap", such as increased variance in the yearly burnt area, the occurrence of extreme fire years, or larger individual fire sizes. This outcome reflect the design of the fuel suppression module within the REMAINS model, as well as interactions among model parameters such as fuel thresholds, suppression resource distribution, and the distribution of yearly burned area.

However, our experiment clearly shows an element often overlooked in the rewilding debate: the role of fire as a process that can "rejuvenate" the landscape and thereby alter the trajectory of carbon stocks. The rejuvenation rule (i.e., reducing one age class for non-stand-replacing fires and triggering "shrub-to-…" transitions for forests in the first age class) provides a compact representation of the fact that, even without complete conversion, fires reduce surface fuels and biomass (here proxied by age). This generates effects that can appear "beneficial" for risk mitigation while "negative" for

carbon sink strength in the short term—and vice versa. Trends in mean stand age (for both broadleaf and conifer forests) and the PCA are particularly instructive. The PCA indicates that the primary axis is dominated by forest age, and that the relationship between age and BA shifts over the simulation period: initially, age and BA tend to load in the same direction, whereas after approximately 80 years they become opposed — consistent with the mechanism of fire-induced rejuvenation i.e., (more area burned → more cells losing age classes → lower mean age). From a carbon stock perspective, this implies that the ecoregions most exposed to high BA may never reach (or may fail to maintain) the mature forest stages that maximise stocks and the accumulation of deadwood and litter. Therefore, the carbon-sink potential of Alpine rewilding is not determined solely by the extent of the rewilded area, but also by the likelihood that these areas remain in older age classes long enough without being partially or fully reset by disturbance.

A comparison between FSR_DP and FSR_DIP provide additional insights. FSR_DIP tends to maintain lower mean stand ages (a combined effect of conversion to cropland for the agromosaic and implementation of prevention measures) while also keeping BA more contained. This pattern reflects a structural compromise typical of fire-smart policies: sacrificing a share of widespread proforestation and ageing to increase landscape discontinuity and enhance fire controllability. This trade-off is central to the integrated planning that the REWILD-FIRE project aims to support. In mountain systems where the goal is a stable net carbon sink by 2060, it may be rational to prioritise resilience (i.e., reducing the probability of catastrophic losses) even at the cost of locally limiting forest maturation. However, while the effect on reducing forest age was neat, the corresponding effect on BA reduction was less pronounced than anticipated. Specifically, we expected a stronger leverage on BA reduction from the indirect prevention strategy, which converts 5% of young forests to croplands, than what was observed in the simulations.

5.3 Model limitations

The REWILD-FIRE experiments have some methodological limitations that should be considered in future development and tests: (i) the FWI–BA relationship remains weak and sensitive to smoothing (monthly/seasonal) and to a short observational window; (ii) uncertainty across climate models is large; and (iii) non-climatic factors (ignitions, suppression capacity, future land-use changes not climatically determined) are not fully endogenous in the empirical component. Nevertheless, because REWILD-FIRE is designed to compare policy scenarios “under the same climatic drivers” and to quantify relative differences among strategies, this framework is appropriate. Rather than predicting the timing of the next major fire, it evaluates which combinations of rewilding, management, and prevention make the system less prone to high BA and more robust under increasing hazard.

The results are highly sensitive to model parameterization. Adapting the REMAINS model to the specific needs of the REWILD-FIRE project further increased the complexity of interactions among the different model functions, making parameter calibration particularly challenging when aiming to reproduce dynamics observed in the real world (e.g. the fire-fighting trap). Understanding the effect size of interactions among fuel suppression and spread rate parameters, and reductions or increases in flammability driven by management or forest ageing makes it almost impossible to predict the emergent patterns after 80 years of simulation. Nevertheless, this aspect is itself of great interest, as a decision support system such as REMAINS is also intended to reveal potentially unexpected trajectories and to support reasoning about policy interactions depending on territorial characteristics.

In conclusion, the results of Deliverable 3.1 coherently support the project objectives. In the Alps, where reforestation and proforestation are already reshaping the landscape mosaic and where an

increase in disturbances is plausible, the key question is not “how much area can we rewild?”, but rather “how can rewilding be spatially planned to maximise a stable net carbon sink once expected losses from wildfires are accounted for?”. The evidence indicates that fire-smart strategies (i.e., selecting low-hazard areas for rewilding, direct prevention through firebreaks, and—where feasible—strengthening agromosaics) are more likely to reduce BA and thereby safeguard, over time, the climate benefits of rewilding. Such strategies help prevent biomass accumulation from becoming a source of systemic vulnerability.

References

Aquilué, N., Fortin, M.-J., Messier, C., & Brotons, L. (2020). The Potential of Agricultural Conversion to Shape Forest Fire Regimes in Mediterranean Landscapes. Ecosystems, 23(1), 34–51. https://doi.org/10.1007/s10021-019-00385-7

Ascoli, D., Russo, L., Giannino, F., Siettos, C., & Moreira, F. (2018). Firebreak and fuelbreak. In Encyclopedia of wildfires and wildland-urban interface (WUI) fires (pp. 1–9). Springer. https://doi.org/10.1007/978-3-319-51727-8_70-1

Duane, A., Aquilué, N., Gil-Tena, A., & Brotons, L. (2016). Integrating fire spread patterns in fire modelling at landscape scale. Environmental Modelling & Software, 86, 219–231. https://doi.org/10.1016/j.envsoft.2016.10.001

Moreira, F., Ascoli, D., Safford, H., Adams, M. A., Moreno, J. M., Pereira, J. M., ... & Fernandes, P. M. (2020). Wildfire management in Mediterranean-type regions: paradigm change needed. Environmental Research Letters, 15(1), 011001. https:// 10.1088/1748-9326/ab541e

Moris, J. V., Gamba, R., Arca, B., Bacciu, V., Casula, M., Elia, M., Malanchini, L., Spadoni, G. L., Vacchiano, G., & Ascoli, D. (2024). A geospatial dataset of wildfires in Italy, 2007-2022 (Version 1.0). Zenodo. https://doi.org/10.5281/ZENODO.11528284

Perino, A., Pereira, H. M., Navarro, L. M., Fernández, N., Bullock, J. M., Ceaușu, S., Cortés-Avizanda, A., van Klink, R., Kuemmerle, T., Lomba, A., Pe’er, G., Plieninger, T., Rey Benayas, J. M., Sandom, C. J., Svenning, J.-C., & Wheeler, H. C. (2019). Rewilding complex ecosystems. Science, 364(6438), eaav5570. https://doi.org/10.1126/science.aav5570

Spadoni, G. L., Moris, J. V., Vacchiano, G., Elia, M., Garbarino, M., Sibona, E., Tomao, A., Barbati, A., Sallustio, L., Salvati, L., Ferrara, C., Francini, S., Bonis, E., Dalla Vecchia, I., Strollo, A., Di Leginio, M., Munafò, M., Chirici, G., Romano, R., … Ascoli, D. (2023). Active governance of agro-pastoral, forest and protected areas mitigates wildfire impacts in Italy. Science of The Total Environment, 890, 164281. https://doi.org/10.1016/j.scitotenv.2023.164281

Spadoni, G. L., Moris, J. V., Kirschner, J., De Miguel, S., Menor, I. O., Passamani, C., Terzuolo, P., Gottero, F., Le Moguédec, G., Ascoli, D., & Motta, R. (2026). Active and passive forest management: Effects on ecosystem services across protected and unprotected areas in a Southern European regional context. Forest Ecology and Management, 602, 123387. https://doi.org/10.1016/j.foreco.2025.123387

Valese, E., Conedera, M., Held, A. C., & Ascoli, D. (2014). Fire, humans and landscape in the European Alpine region during the Holocene. Anthropocene, 6, 63-74. https://doi.org/10.1016/j.ancene.2014.06.006